



DIVERSE OLIVINE TYPES IN LAVA OF THE 1959 ERUPTION OF KILAUEA VOLCANO AND THEIR BEARING ON ERUPTION DYNAMICS

By Rosalind Tuthill Helz

ABSTRACT

The lava of the 1959 eruption of Kilauea Volcano, containing about 20 weight percent olivine, is the only picritic lava erupted in the summit area in historical time. The olivine population can be divided into several distinct classes: (1) irregular, blocky crystals (1–12 mm long), many of which contain multiple planar extinction discontinuities, which appear to be deformation features; (2) euhedral or skeletal crystals (0.5–5 mm long); (3) round or otherwise strongly resorbed grains; (4) angular or conchoidal fragments; and (5) subhedral crystals containing sulfide-bearing inclusions. Also present are dunitic aggregates, some with deformed or annealed textures, and rare olivine megacrysts.

Olivine in drill core from Kilauea Iki lava lake, quenched as much as 22 years after the eruption, has the same petrographic features seen in eruption samples or early lake samples. In particular, the deformation features in olivine have survived 22 years at 1,140–1,190 °C.

Olivine phenocrysts in samples of eruption pumice have core compositions of $Fo_{83.5-88.7}$ and contain 0.10–0.25 weight percent NiO. Zoning is moderate (≤ 3 percent Fo within most crystals); normally and reversely zoned crystals are about equally abundant. There is no correlation between petrographic class and core composition or style of zoning. This variable but moderate zoning seen in olivines in the eruption pumices is not preserved in olivines in drill core from the lake. Lake olivine is all normally zoned, varying by 5 percent Fo or more, and appears to have re-equilibrated with the melt during slow cooling.

The eruption samples are, for the most part, poorly equilibrated. Disequilibrium features observed include: (1) compositional heterogeneity in glasses (away from olivines); (2) presence of a boundary layer of MgO-poor glass near 30 percent of the olivine grains analyzed; (3) widespread occurrence of partially resorbed olivines, in all classes; (4) presence of reversely zoned, unzoned and (or) normally zoned olivines in the same thin section; (5) presence of olivines of very different core compositions in the same section; and (6) presence of olivines of different rim compositions in the same section. These features appear to record mixing immediately before or during the eruption. In particular, the resorption of olivine, seen in grains of all classes, at all but the earliest stages of the eruption, is interpreted as resulting from mixing of thermally disparate magmas, in which the hotter component was dominant.

Many aspects of this eruption are unusual for a Kilauean summit eruption, including: (1) High olivine content; (2) very magnesian glasses, recording high eruption temperatures; (3) the presence of deformed olivine, as single grains or in aggregates, like that commonly found in Hawaiian alkalic rocks; (4) occurrence of rare olivine megacrysts; (5) presence of olivine

with sulfide-bearing inclusions; and, perhaps, (6) presence of reversely zoned olivines. These features can be explained by a model in which one of the two mixing components of the eruption, previously defined by Wright (1973), came directly from the mantle, without being stored for a significant time in the shallow summit reservoir. The lava component erupted from the east end of the initial fissure appears to represent this juvenile component. The ascent rate of this component from its source at a depth of 45–60 km is estimated to be 0.6–0.8 cm/s. This rate is sufficient to entrain the largest olivine grains and dunitic aggregates found in the 1959 lavas.

INTRODUCTION AND HISTORICAL BACKGROUND

The 1959 summit eruption of Kilauea Volcano was unique in the history of the Hawaiian Volcano Observatory (HVO) and of Kilauea in that it was the first major eruption for which most of the array of modern volcano-monitoring techniques now available was used. This eruption lasted from November 14 to December 20, 1959, and formed a conspicuous cinder cone (Puu Puai) and a large lava lake in Kilauea Iki pit crater (see fig. 25.1). The eruption consisted of seventeen phases of high fountaining and lava output, separated by periods of quiescence, during which some of the erupted material drained from the lake back down the throat of the main vent. HVO personnel made detailed records of this eruptive activity, its timing and patterns, including fountain heights and temperatures, and the depth of filling of the pit crater. The pumice and lava were then studied petrographically and chemically. These results were published in a series of professional papers (Murata and Richter, 1966a; Richter and Murata, 1966; Richter and others, 1970) that, taken together, give a very detailed picture of the eruption. In addition, Kilauea Volcano had been monitored seismically for several years before 1959; also, summit deformation before and during the eruption was monitored using the tiltmeter network established in 1957. Descriptions of the relationship between earthquake activity, summit deformation and the 1959–60 eruptions of Kilauea, by Eaton (1962) and Eaton and Murata (1960), constituted a quantum jump in our understanding of the physical behavior of active volcanoes.

The lava lake formed during the 1959 summit eruption has also been much studied. The upper crust of the lake has been drilled repeatedly (in 1960, 1961, 1962, 1967, 1975, 1976, 1979, and

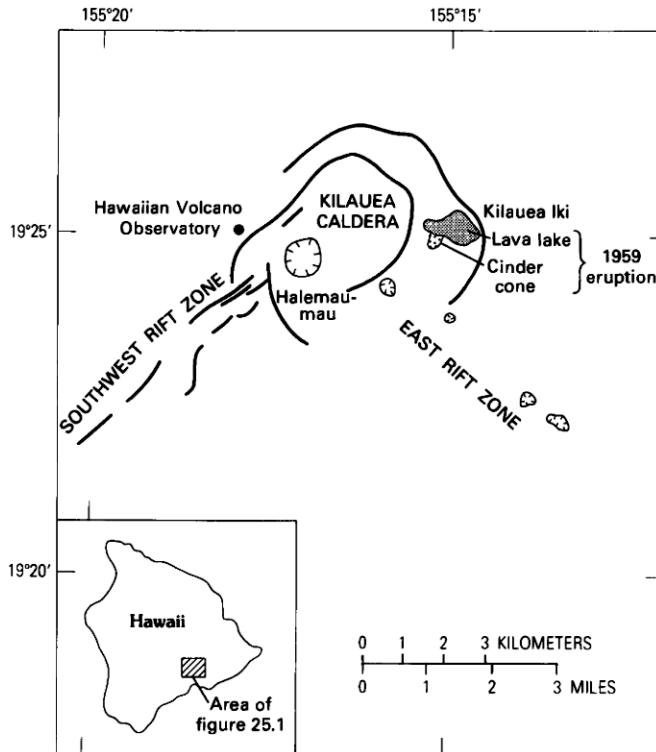


FIGURE 25.1.— Index map of the summit area of Kilauea Volcano, showing the location of Kilauea Iki lava lake and the 1959 cinder cone relative to the main caldera and the upper east rift zone of Kilauea.

1981), resulting in almost 1,200 m of drill core. Richter and Moore (1966) present a detailed petrographic and chemical description of the 1960–62 core. Partial data on petrography and (or) chemistry for the drill core recovered in 1967–1981 may be found in Helz (1980), Luth and Gerlach (1980), Luth and others (1981), Helz and Wright (1983), Helz and others (1984), and Helz (1984). The thermal history of the lake has also been monitored from the earliest days; Helz and Thornber (in press) give a partial summary of that literature. Lastly, the lake has been the object of several geophysical investigations, such as those of Zablocki and Tilling (1976), Chouet and Aki (1981), Hardee and others (1981), and Hermance and Colp (1982).

The 1959 summit lava is unique in several respects, the most conspicuous of which is its olivine content: it is the only picritic basalt erupted at or near Kilauea's summit in historical time. The average MgO content of the eruption pumice was estimated by Wright (1973) to be 15.43 percent by weight, which corresponds to about 20 percent by weight olivine crystals. Other historical eruptions with comparable olivine content have occurred on the rift zones, for example, the 1840 east-rift eruption (see analyses in Macdonald, 1944; Wright and Fiske, 1971). Other young summit eruptions have 7.0–8.5 percent MgO and correspondingly smaller amounts of phenocrystic olivine (Wright, 1971).

Consequently, the eruption pumice and the 1959 lava lake contain an enormous population of olivine crystals, occurring singly and in aggregates. This paper presents the results of a petrographic and chemical study of selected olivine crystals and aggregates, both in eruption pumice and in drill core from the lava lake. The study supplements earlier work on the eruption (cited above) by providing detailed electron microprobe data on a large suite of eruption samples. A limited amount of microprobe data on the 1959 eruption pumices has already been published (Leeman and Scheidegger, 1977; Harris and Anderson, 1983), but coverage of the eruptive suite was very incomplete.

ACKNOWLEDGMENTS

This paper builds on the past and present work of many people who have studied the 1959 eruption. In particular, I would like to thank J.G. Moore of the United States Geological Survey (USGS), Menlo Park, for access to his thin sections of submarine east-rift lava and T.L. Wright (USGS, Hawaiian Volcano Observatory) for access to his collection of thin sections of subaerial Kilauea lava. B.C. Hearn (USGS, Reston) and S.H. Kirby (USGS, Menlo Park) helped with the interpretation of the textures of the annealed olivine aggregates. In addition, I have benefited from conversations with D.A. Clague, J.P. Eaton, P. Delaney and S.W. Kieffer, all of the USGS, A.T. Anderson, Jr. of the University of Chicago, and C.-Y. Chen of the University of Illinois at Urbana. Lastly, I wish to thank B.C. Hearn and M.P. Ryan for constructive reviews of the manuscript.

SAMPLING AND ANALYTICAL PROCEDURES

SAMPLE SELECTION

The 1959 summit eruption consisted of 17 distinct phases. These phases, and the variations of lake level with time, are described in detail in Murata and Richter (1966a) and Richter and others (1970) and are summarized in figure 25.2. During each phase, eruptive materials were sampled, often both pumice from the fountain and flow material from the edge and upper crust of the lava lake. In selecting a subset of samples for this study, preference was given to pumice samples, because they were quenched much faster than flow samples, and to samples previously studied, especially those for which a bulk analysis was presented in Murata and Richter (1966). The collection dates of samples examined petrographically is indicated by the dots along the curve in figure 25.2. Although samples from only twelve of the seventeen phases were checked, they are fairly evenly distributed in time throughout the eruption.

In addition to these eruption samples, I have examined 600 thin sections of drill core from the lava lake. The drill-core sections contain all the types of olivine seen in the eruption samples. In addition, I found in the drill core two olivine megacrysts and a dozen dense polycrystalline olivine aggregates of distinctive texture. These unusual aggregates and megacrysts, of types not seen in the eruption pumice, are the only lake samples that will be discussed in detail in this paper.

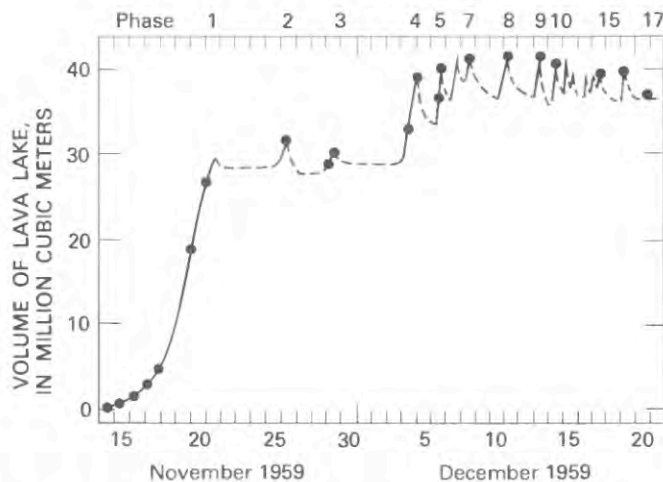


FIGURE 25.2.—Volume of Kilauea Iki lava lake versus time (after Richter and Moore, 1966, fig. 3). Decrease in lake volume at the end of each phase represents drainback down the eruptive vent. Each dot corresponds to a sample examined in this study. Phases represented in this study are numbered along the top of the diagram.

PETROGRAPHIC METHODS

All thin sections have been examined in transmitted light. All polished sections have also been checked in reflected light to verify the identification of opaque and near-opaque phases. No universal-stage work has been done.

In addition to the thin-section work, the drill core from the lake has been examined macroscopically in detail, with emphasis on the size and distribution of olivine phenocrysts. The results of this work are presented in Helz (1980), Helz and Wright (1983), and Helz and others (1984) and form part of the background to the present paper.

ANALYTICAL METHODS

Olivine and glass analyses were obtained using an ARL-SEMQ nine-channel electron microprobe. Operating conditions were an accelerating voltage of 15 kV and a beam current of 0.1 μ A. Natural mafic silicates and basaltic glasses were used as standards. Counting times were 40 s for most major elements, 20 s for some of the minor elements (Ti, Cr, P, and K in glass; Ni and Cr in olivine). All data were reduced using a modified Bence-Albee routine (Bence and Albee, 1968; Albee and Ray, 1970). In addition, the glass analyses were renormalized, using a glass of known composition, following the method of Melson and others (1976). The glass selected for this was sample 69-1-22 from the 1965 Makaopuhi lava lake (Wright and Okamura, 1977). The revised analysis of Jarosewich and others (1979) was used for the renormalization procedure. This process eliminates minor day-to-day variations in analyses caused by slight shifts in the instrument and produces a data set of great internal precision. The accuracy of the analyses, which depends on the uniformity of the standards, the accuracy of the standard analyses, and of the Bence-Albee correc-

tions, is not affected by the renormalization procedure. All analyses reported correspond to the composition of a single point unless the number of points included is specified.

CLASSIFICATION OF OLIVINES

The olivine in the lava of the 1959 Kilauea eruption is not only abundant but quite varied petrographically. The earliest description is that of Richter and Murata (1966), who described three classes of olivine: euhedral, rounded, and skeletal. The euhedral and skeletal olivine they reported to be fairly iron-rich (Fe_{82}), whereas the larger, blocky grains with rounded corners were more magnesian (Fe_{87-88}). The compositions were determined by X-ray techniques. Richter and Murata further remarked that the larger, rounded grains were obviously out of equilibrium with their present host liquid just before quenching, whereas the more iron-rich euhedral grains appeared to have the equilibrium olivine composition.

Based on examination of drill core from the lake, Helz (1980) divided the olivine phenocryst population in the lake into two groups. Type 1 were large, blocky crystals, the overall form of which was irregular. These commonly, but not always, contain multiple planar extinction discontinuities, bounding kink-bands, or subgrains with rectangular boundaries; similar features have been described by Kirby and Green (1980) in olivine in dunite xenoliths from Hualalai Volcano. Type 2 grains, in this classification, were smaller, euhedral olivines, which were free of deformation features. Type 2 olivine is more abundant than type 1 by a ratio of roughly 5:1.

Further study of samples from both the lava lake and the eruption pumice has led to the following five-fold classification:

(1) Class 1 (formerly type 1) consists of large grains (1–12 mm long), generally blocky in form, but irregular in overall outline, as described in Helz (1980). They commonly contain planar extinction discontinuities, bounding kink-bands, which extend all the way across the crystal (see figs. 25.4A–B, 25.5A). More rarely, the subgrains may be rectangular (see fig. 25.5B). Grains of this class rarely contain melt inclusions. Although planar extinction discontinuities may be quite abundant in a given grain, the total amount of strain involved is usually not large. The extinction position of different parts of the grains never varies by more than 15° of rotation and the usual range is 5° – 10° . These grains may exhibit local rounding or resorption at their edges. If resorption is present, the subgrain boundaries are preferentially resorbed by the melt (as in figs. 25.4A, 25.5A). Olivine grains in this class are the most conspicuous in any given thin section (see fig. 25.3).

(2) Class 2, containing all euhedral and skeletal grains (see figs. 25.3, 25.4C and 25.5C), is the most abundant class of olivine. The distinguishing feature of this class is that the form of the grains suggests that they have grown from a melt in the recent past. Minor rounding of tips and corners of grains may occur, but in general class 2 olivine exhibits much less resorption than class 1 grains do. They are completely free of multiple planar extinction discontinuities. They commonly contain melt inclusions, most often a single large inclusion, of negative crystal form, in the center of the grain. Grains

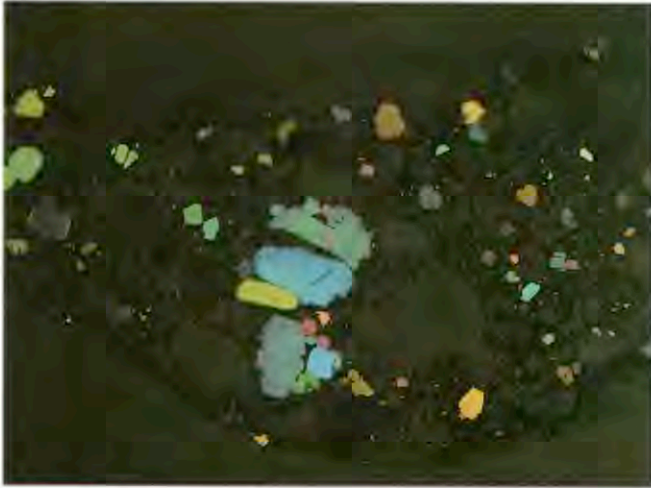


FIGURE 25.3.—Eruption sample Iki-24, from phase 9 of the 1959 eruption. All birefringent grains are olivine; matrix is moderately vesicular brown glass. Note large range in size that exists for both olivine and vesicles. Nicols partly crossed. Field of view is 2.2 cm across.

of this type are commonly 0.5–2 mm long, but they may reach 5 mm in length. A large skeletal grain is shown in figure 25.4D; skeletal grains of this size are rare in the 1959 lavas.

(3) Class 3 includes a small population of grains whose shapes have been so extensively modified by resorption that they cannot be assigned to group 1 or 2 on the basis of shape. Most class 3 grains are almost perfectly rounded. More rarely they may be amoeboid, but are never skeletal. These grains do not contain kink-bands; any grain with such features, even though strongly rounded, has been put in class 1.

(4) Class 4 includes rare angular or conchoidal fragments of olivine. Some care is needed to distinguish between broken pieces of olivine and crystals that have odd shapes because they have been sectioned obliquely. Nevertheless, there are a few grains of olivine that are clearly bounded by fracture surfaces. This class provides evidence for local brittle failure of olivine under conditions quite different from those under which the deformation features seen in class 1 olivine formed. Some of these angular fragments may be slightly modified by resorption (see fig. 25.4C). Others have survived for decades in the lake without significant resorption or overgrowth of olivine (see fig. 25.5D).

(5) Class 5 olivine grains are those containing swarms of inclusions of opaque minerals and pale glass, in which the opaques consist partly or entirely of sulfide. Chromite (or chromian spinel) is the other opaque phase that may be present. Class 5 grains are very rare, melt-bearing inclusions in most grains being sulfide-free. Sometimes the entire core of the olivine grain is so charged with inclusions that it looks dirty in thin section. More often, the inclusions occur only in patches within an otherwise clear grain. Inclusions also occur as a continuous necklace, separating a clear core and a clear rim. Examples of these various types are shown in figures 25.4E and 25.5E. Grains in this class are usually small (1–4 mm long) and are equant but not conspicuously euhedral in

outline. A few class 5 grains contain planar extinction discontinuities, but most are undeformed. The presence of included sulfide is the crucial feature in assigning a grain to this class. Some olivine grains have inclusion swarms similar to the class 5 swarms in all respects, except that they lack sulfide. These grains have been excluded from class 5 as presently defined, though more detailed work on their inclusions might justify extending this class to include them.

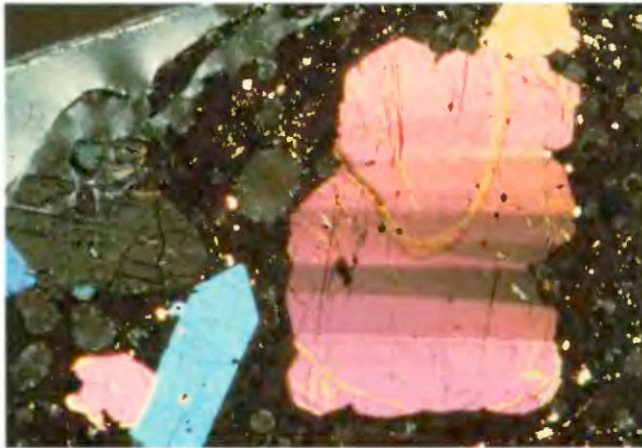
This five-fold classification was first published in Helz (1983). Almost simultaneously, and quite independently, Schwindinger and others (1983) published a different classification scheme for olivine in the 1959 lava. Schwindinger and coworkers leached the olivine grains out of the glass of several samples of eruption pumice to view them in three dimensions. Their classification thus emphasizes three-dimensional form and surface morphology. Also, they worked exclusively with eruption pumice. These differences in scope and technique have led inevitably to different classification schemes. The two schemes are not in conflict, however; rather, the two studies complement each other.

The present classification scheme was developed by looking at olivine as it appears in thin section, that is, in two dimensions. I have considered chiefly the overall form of the grain (complexly blocky, euhedral, round, fragmental) and the presence of certain internal features (multiple planar extinction discontinuities, swarms of sulfide-bearing inclusions) in assigning a grain to a given class. Features not used here to classify grains include: Size of grain; presence or absence of inclusions of chromite or brown glass; and presence or absence of minor or local resorption. Certain classes do exhibit group characteristics with respect to this set of features. For example, class 1 grains tend to be larger than any other type. Inclusions of brown basaltic glass are very common in class 2 grains, and rare in all other classes. However, this clustering of additional traits is a matter of observation, and not part of the classification process.

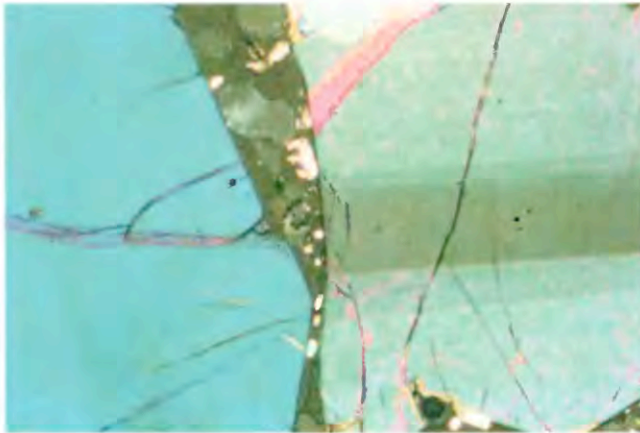
With so many types of olivine present, the possibility obviously arises that only some classes of crystals (for example, class 2) are cognate with the host, whereas others (perhaps class 1) may be largely xenocrystic. As will become evident below, there are many gradations between cognate and xenocrystic, and so these terms will be little used in this paper. Instead, the term phenocryst is used to mean any olivine grain big enough to see with the unaided eye, without genetic implications, while the terms grain or crystal may include smaller olivine grains as well.

PETROGRAPHY OF THE ERUPTION PUMICE

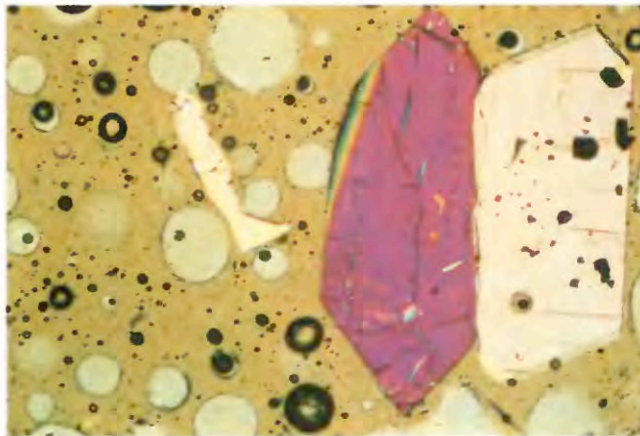
The eruption samples examined in this study are listed in table 25.1, together with their dates of collection and petrographic notes on the olivine present. Two sample designations are given. The first is the collection number assigned in the field, which will be used in this paper. The second number (S-number in parentheses) is the number used in Murata and Richter (1966a) and Richter and Murata (1966); it is reproduced here to facilitate comparison with those papers. Some samples investigated here were not analyzed in



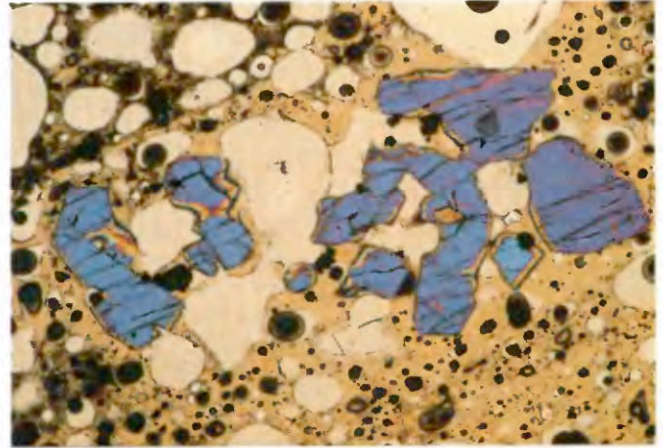
A



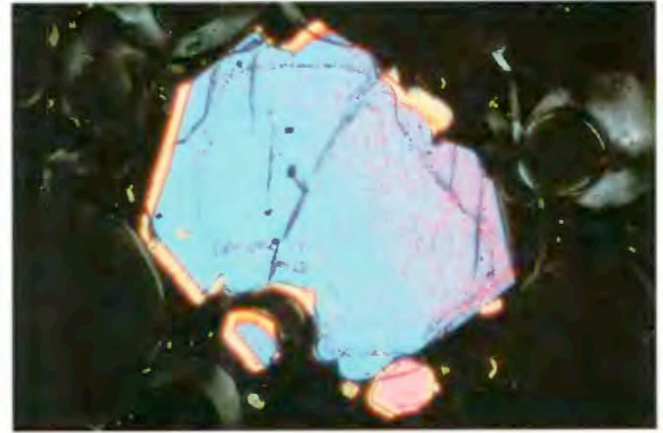
B



C



D



E

FIGURE 25.4.—Representative olivine grains from the eruption pumice of the 1959 Kilauea eruption. **A**, Deformed (class 1) olivine grain, 2 mm long from Iki-21 (phase 8). The edges are resorbed and show preferential resorption along the planar extinction discontinuities bounding the kink-bands. Two euhedral (class 2) grains are visible to the left. Crossed nicols. **B**, Deformed (class 1) olivine grain (right), showing relationship between the curved (possibly bent?) edge of the grain and the position of the extinction discontinuities, along an edge where resorption has not occurred. This grain, from Iki-24, is visible in the center of figure 25.3. Field of view 2 mm across. Crossed nicols. **C**, Euhedral (class 2) and fragmental (class 4) olivine grains in Iki-7 (phase 1). The euhedral grains are 1 mm long. Nicols partly crossed. **D**, Coarse skeletal (class 2) olivine grain, 3 mm in length, in Iki-21 (phase 8). Such grains are very rare in the 1959 lava. Nicols slightly crossed. **E**, Class 5 olivine (1 mm long) with necklace of tiny inclusions, from sample Iki-32 (phase 15). The edge of this crystal shows local resorption (cusped edges) but is euhedral elsewhere around its rim. Nicols partly crossed.

the earlier studies, and therefore have no S-numbers.

All samples in table 25.1 contain abundant brown glass, mostly very fresh and clear, but locally charged with fine-grained opaques. All glasses are quite vesicular, some of them so vesicular that less than a third of the area of the thin section is glass and crystals. A typical olivine-rich, moderately vesicular eruption sam-

ple is shown in figure 25.3. All of the birefringent material in this section is olivine; clearly the size range of olivine present is very large.

The crystalline material present in the eruption pumice consists almost entirely of olivine plus chromite. Both phases are always present; there are few chromite-free olivine grains and no chromite-free samples. Chromite occurs principally as inclusions in olivine; most crystals not included in olivine are immediately adjacent to

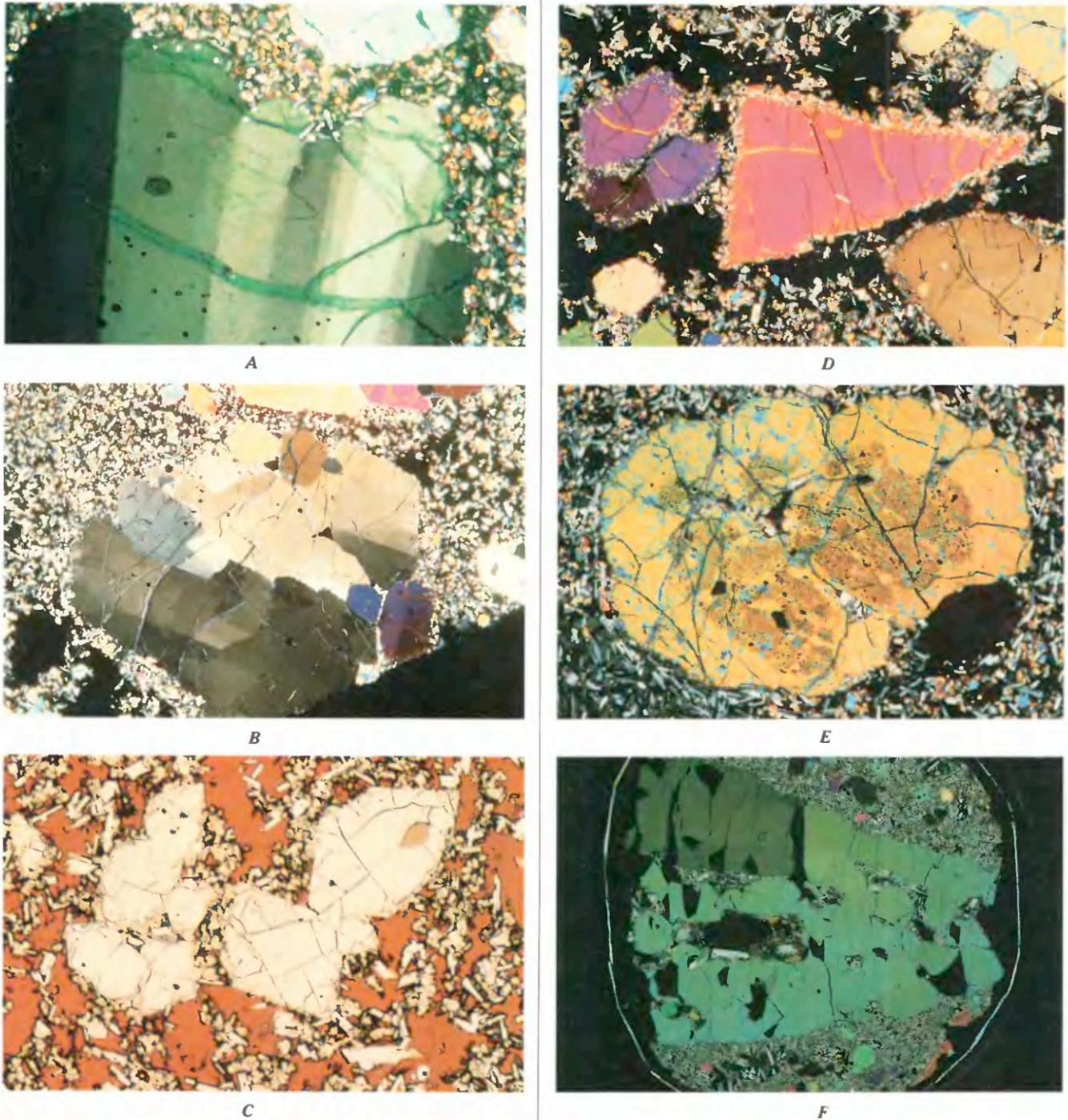


FIGURE 25.5.—Representative olivine from Kilauea Iki lava lake. **A**, Deformed (class 1) olivine grain from KI81-2-226, quenched from 1,140 °C in 1981. It has multiple planar extinction discontinuities and cusped margins like the grain in figure 25.4A. Part of grain visible is 2 mm long. Crossed nicols. **B**, Deformed (class 1) grain in aggregate KI79-1-189.0(b), quenched from 1,130–1,135 °C in 1979. The olive-green grain shows rectangular subgrain boundaries instead of planar extinction discontinuities extending across the whole grain. This grain is 5 mm long. Black area at lower right is the edge of the rock section. Crossed nicols. **C**, Euhedral (class 2) olivine grains from KI76-1-149.1, quenched from 1,105 °C in 1976. These are grouped into clusters of 2–3 grains each. Smaller crystals are groundmass phases, including olivine, augite, and plagioclase, in brown glass. Field of view 3 mm across. Plane-polarized light. **D**, Fragmental (class 4) olivine

grain from sample KI75-1-145.1, quenched from 1,120 °C in 1975. All surfaces of the pink triangular grain are slightly conchoidal. This grain is 5 mm long. Class 1 (yellow grain, lower right) and class 2 (purple grains to left) olivine phenocrysts are also visible. The glass is at extinction. Crossed nicols. **E**, Class 5 olivine phenocryst (3 mm across) with inclusion-rich core, from sample KI81-1-306.7, quenched from 1,085 °C in 1981; smaller, attached grain is at extinction. Crossed nicols. **F**, Olivine megacryst from sample KI76-2-20.5. It is mounted on a glass slide, just visible in the picture, which is 2.54 cm across. The grain is somewhat skeletal, with former melt inclusions now visible as areas of mesostasis. Irregular black areas within the crystal are the result of fragmentation and plucking during sectioning. Faint extinction discontinuities (visible in upper part of crystal) are present throughout the grain. Crossed nicols.

TABLE 25.1.—Samples of 1959 eruption pumice investigated

Sample	Phase of eruption	Date	Type of sample	Olivine classes present	Resorption observed?	Kink bands present in olivines?	Types (numbers) of sections examined
Iki-1(S-2)	1	11/14/59	Flow	2	No	No	TS, PTS
Iki-58(S-1)	1	1/14	Flow	2	No	No	TS, PTS
Iki-42	1	1/16	Flow	2	No	No	TS(2)
Iki-2(S-4)	1	11/17	Pumice	2	No	No	TS
Iki-22 (S-5)	1	11/18	Pumice	1,2,3	Yes	Yes	TS, PTS
Iki-44 (S-7)	1	11/20	Pumice	1,2,3	Yes	Yes	TS, PTS
Iki-5 (S-8)	1	11/21	Pumice	1,2	No	Yes	TS
Iki-7 (S-9)	1	11/21	Pumice	1,2,3,4	Yes	Yes	TS, PTS
Iki-8(S-10)	2	11/26	Flow	1,2	Yes	Yes	TS
Iki-11(S-11)	2	11/26	Pumice	1,2,3,5	Yes	Yes	TS, PTS
Iki-9(S-12)	3	11/28	Pumice	2	Yes	No	TS, PTS(2)
Iki-10(S-13)	3	11/29	Pumice	2	Yes	No	TS
Iki-12(S-14)	4	12/4	Flow	2	No	No	TS
Iki-13(S-15)	4	12/5	Pumice	1,2,3,4	Yes	No	TS, PTS
Iki-14(S-16)	5	12/6	Pumice	1,2,4,5	Yes	Yes	TS, PTS
Iki-15(S-17)	5	12/7	Pumice	1,2	Yes	Yes	TS
Iki-19(S-18)	7	12/8	Pumice	1,2,3,5?	Yes	Yes	TS
Iki-20	7	12/8	Pumice	2,5	Yes	No	PTS
Iki-21(S-19)	8	12/11	Pumice	1,2,4,5	Yes	Yes	TS, PTS
Iki-24	9	12/13	Pumice	1,2,4	Yes	Yes	PTS
Iki-36	9	12/13	Pond Surface	1,2,4	Yes	Yes	TS(2)
Iki-26(S-21)	10	12/14	Pumice	1,2,3	Yes	Yes	TS, PTS
Iki-32(S-22)	15	12/17	Pumice	1,2,3,5	Yes	Yes	TS, PTS
Iki-33(S-24)	16	12/19	Pumice	1,2	Yes	Yes	TS, PTS
Iki-38(S-25)	17?	12/19?	Ooze	1,2	No	No	TS

olivine. Crystals of chromite occurring in the glass, at some distance from olivine, are rare. This pattern of association of olivine and chromite suggests that spinel nucleates on olivine, whenever possible.

A few eruption samples also contain minor amounts of fine-grained augite, with or without tiny laths or plates of plagioclase. These phases occur in all of the earliest phase 1 pumice samples (Iki-58, Iki-1, Iki-42) plus some phase 2 and 3 samples (Iki-11, Iki-9). These minerals are never sufficiently coarse grained to be considered phenocrystic. They do not survive in recognizable form in the lake (Helz, 1980), but must make up part of the groundmass.

As can be seen in table 25.1, the petrographic character of the olivine in the eruption pumice varies with time. The early phase 1 samples (Iki-58, Iki-1, Iki-42, Iki-2) contain only minor amounts of euhedral class 2 olivine showing little or no resorption. Lava temperature evidently increased during this period, however, as the latest of this series of samples does not contain the tiny augite \pm plagioclase crystals seen in pumice erupted on November 14-16. On November 18, 1959, the olivine content of the lava

increased and the olivine assemblage became more complex, now including representatives of classes 1, 2, and 3. This situation persisted to the end of the first phase, with some fragmental olivine (class 4) occurring in the latest sample (see fig. 25.4C).

Phase 2 samples also have a complex olivine assemblage, including the earliest known class 5 olivine. Phase 3, by contrast, marks a reversion to a depleted olivine population like the early phase 1 pumice, but with more rounding of the olivine. An early phase 4 sample is similarly olivine-poor, but later phase 4 and the phase 5 samples again contain a complex olivine assemblage, which contains the first fragmental olivine seen since the end of phase 1.

Phase 6 is not represented, but phase 7 pumice continues to have a very complex olivine assemblage, containing all classes of olivine except the fragmental class 4. Phases 8 and 9 contain abundant and very variable olivine (see figs. 25.3, 25.4A-B), including class 4 fragments, but without any class 3 (round or strongly resorbed) grains. These are the last eruption samples known to contain fragmental olivine. In phases 10 and 15, rounded

class 3 olivine reappears, but class 4 olivine is absent. Later samples from phase 16 and 17(?) contain abundant olivine, but it is, like that in the earliest pumice, less variable in form. In the latest sample, an ooze, the olivine shows neither resorption nor kink-bands; the only other samples like it are the earliest (November 14–17) phase 1 samples.

Thus, the sequence of appearance of the different classes is: first, class 2, followed by 1 and 3, then 4, then 5. Class 3 and class 4 olivine tend not to occur in the same sample: of the eight samples with class 3 grains and 6 samples with class 4 fragmental olivine, only two (Iki-7, Iki-13) contain both classes. Class 5 olivine, the last class to appear, is found in phases 2, 5, 7, 8, and 15 and may occur in association with any of the other classes. The sequence of disappearance, as the eruption went on, was: first, 4, then 3 and 5, leaving only 1 and 2 present in the last phase.

Certain of these classes are uncommon, and it might be thought that the apparent gaps in the occurrence of classes 3, 4, and 5 would disappear, if more thin sections were examined. For many samples, however, more than one section is available already, and the olivine population is almost always the same in both sections. Thus, it appears that the occurrence of class 3, 4, and 5 olivine as reported in table 25.1 is not an accident of sectioning but a characteristic of particular samples.

PETROGRAPHY OF OLIVINE PHENOCRYSTS AND MEGACRYSTS IN THE LAVA LAKE

The same five classes of olivine that occur in the eruption pumice can be found in samples from the lake. Such samples cannot be related to individual phases, however, because of mixing in the lake, drainback between phases, and re-eruption of some of the same material in later phases. In addition to these complications, there has been significant redistribution of olivine within the lake after it crusted over, as discussed in Helz (1980). The dominant process was probably gravitative settling, as the coarser class 1 olivine grains have been affected more than the smaller class 2 phenocrysts. For these reasons, it is not possible to develop an olivine stratigraphy for the lake that would correlate with the time sequence observed in table 25.1. Post-eruptive redistribution of olivine has produced essentially three zones in the lake: an upper, olivine-rich zone down to a depth of 18 m, an olivine-depleted zone from 18–40 m, and a second olivine-rich zone from 40 m down to within 2 m of the bottom of the lake (Helz, 1980; Helz and Wright, 1983; Helz and others, 1984). Both olivine-rich zones contain all five classes of olivine. The olivine-depleted zone generally contains only class 2 grains, which are commonly rounded and may be locally rimmed with pyroxene.

It might be thought that some of the features used to classify olivine in the eruption pumice would disappear during prolonged annealing in the lake. In fact, the only type of grain significantly affected is the skeletal olivine. Skeletal grains do occur in the pumice, though usually only in the microphenocryst size range (<0.5 mm). Lake samples, having cooled more slowly, contain virtually no skeletal olivine. Sample KI79-1-189.0 contains the

only known example of a coarse skeletal olivine in the lake. Typical grains of class 2 lake olivine are shown in figure 25.5C. These look very much like their equivalents in the eruption pumice, as overgrowths of olivine are minor and glass inclusions tend to crystallize later than the melt outside the olivine.

Other types of olivine have also survived as much as 22 years of slow cooling unscathed. For example, figure 25.5A shows a class 1 olivine, with multiple planar extinction discontinuities, and strongly resorbed outline, which is virtually identical to the grain shown in figure 25.4A. The first grain was quenched from 1,198 °C on December 11, 1959 (see table 25.1). The second was quenched from 1,140 °C on April 22, 1981 (Helz and Wright, 1983; Helz and Thornber, in press). The extinction discontinuities have not been removed by annealing, nor have the crystallographically irrational curved surfaces of the resorbed grains healed. Apparently they are very unfavorable sites for further growth of olivine. Fragmental olivine also survives in the lake (see fig. 25.5D), perhaps for the same reason: the broken surfaces are not favorable growth sites, compared with the abundant rational faces and edges available on the class 2 phenocrysts and groundmass olivine.

The distribution of class 5 grains in the lake, which appears to be random, is of particular interest. These grains occur in olivine-rich samples at the edge of the lake, and in the center, at all depths, wherever class 1 grains occur. One of the best examples of this class (fig. 25.5E) is from the bottom of the deepest drill hole in the center of the lake. As indicated in table 25.1, class 5 grains have not yet been observed in any phase 1 samples. The bulk of the lake, however, was erupted during phase 1 and did not drain back down the vent (see fig. 25.2). Therefore, if the apparent absence of class 5 grains from phase 1 is real, the presence of grains of this class throughout the lake, including its most northerly and (or) deepest parts, implies that the bulk of the lake was very well mixed during phases 2–17, and perhaps for some time thereafter, even though there was little net increase in lava in the lake after phase 1.

OLIVINE MEGACRYSTS

The principal reason for considering lake samples in a paper on the dynamics of the 1959 eruption is that the lake contains a sparse population of very large olivine grains and aggregates of olivine, distinct from any observed in the available thin sections of eruption pumice. Perhaps the most curious are the two olivine megacrysts that have been found in the lake. One of these is shown in fig. 25.5F; data on both are presented in table 25.2.

The actual size of these large single crystals, or megacrysts, of olivine is unknown, but the parts of the grains visible in drill core and thin section are 20 mm by 10 mm. Though found at very different levels in the lake, the two grains are so much alike that they look like pieces of the same crystal. Both are wedge-shaped in section and contain as inclusions large areas of glass plus augite, plagioclase, and other groundmass phases. Presumably the original grains were skeletal, with irregular cavities in their cores. Their external form is not euhedral; their present grain boundaries appear to be fracture surfaces, at least in part. Both megacrysts contain abundant planar

extinction discontinuities (as in fig. 25.5F), but the total angle of rotation is very slight in both megacrysts. The planes are decorated with minute inclusions or voids, a style of decoration that is not commonly observed in ordinary class 1 olivine phenocrysts. Megacrysts of this sort have not previously been reported in Kilauean lava.

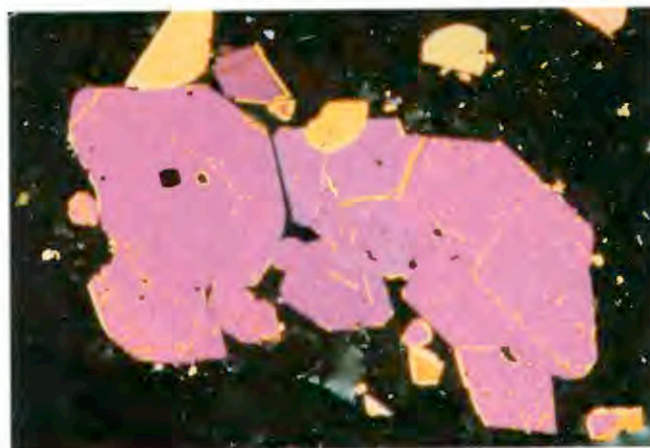
PETROGRAPHY OF OLIVINE AGGREGATES

Schwindinger and others (1983) reported that 95 percent of the olivine in the eruption samples studied by them occur in aggregates. This figure is not unreasonable for other eruption samples as well, but may be a little high for lake samples. Whatever the exact figure, isolated single crystals of olivine are uncommon. Large clots of crystals are also exceptional, however; most clumps of crystals appear, at least in thin section, to consist of 2–6 individual grains (see fig. 25.3).

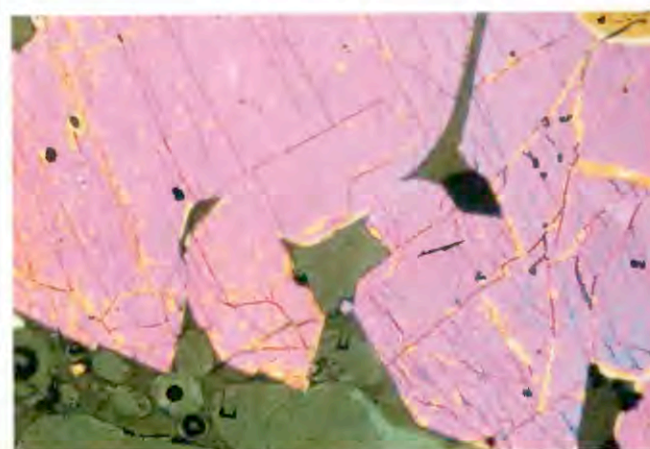
If one considers only the largest aggregates, there are two distinct types present. The more common type of large olivine aggregates consists of relatively open or skeletal clusters of grains, like that shown in figure 25.6A–B. These open clusters consist of class 2 grains, rounded or otherwise, which have a common crystallographic orientation. A subordinate set, rotated 90° from the first set, is not uncommon, but other crystal orientations are rare. The crystals in these open aggregates are not sorted by size (see fig. 25.6B especially). These networks of crystals are open, with glass and vesicles along boundaries and at interstices. Schwindinger and others (1983) studied this type of open aggregate in some detail and recognized several subcategories. They have suggested that these aggregates form by synneusis, the swimming together of crystals suspended in a melt. Similar aggregates are common in the lake; these differ from the one shown in figure 25.6A chiefly in that they contain fewer crystals and less interstitial glass. The significance of these aggregates is that, whatever their exact origin, everything about them suggests that they formed in the presence of abundant melt, most probably in Kilauea's summit reservoir.

The second group of olivine aggregates differs markedly in character from the open, glomerocrystic clots described above. This group, which will be referred to as dense olivine aggregates or dunite aggregates, consists of clusters of non-euhedral olivine, for the most part very tightly interlocked or intergrown. The grains are not oriented crystallographically relative to each other. Such olivine aggregates, or dunite fragments, are uncommon; the one dozen examples known to date are described in table 25.2.

The dunitic aggregates in table 25.2 are from drill core, and so have undergone variable periods of slow cooling in the lake between eruption and quenching. Therefore, table 25.2 includes the dates on which the various samples were drilled and the temperatures from which they were quenched. The temperature estimates are based on the composition of the glass found in the groundmass of the host rock of each sample, using the empirical calibration presented in Helz and Thornber (in press) for Kilauean samples, except for sample KI76–2–20.5, which was collected long after the rock crystallized. For this sample, the temperature (about 100 °C) was



A



B

FIGURE 25.6.—Skeletal olivine aggregate from the 1959 Kilauea eruption. **A**, Aggregate of euhedral grains in sample Iki-33 (phase 16). Note the strong preferred orientation of the crystals. The aggregate is 6 mm long. Crossed nicols. **B**, Close-up of the same aggregate, showing its open nature. Interior grain margins are slightly rounded, exterior margins strictly euhedral.

determined by downhole thermocouple measurement. From these data it can be seen that individual aggregates were stored anywhere from 9 months to 22 years in the lake and quenched from temperatures ranging from 950 °C to 1,140 °C.

It is evident from table 25.2 that these twelve dunitic aggregates are not distinctive in size; most are similar in size to the largest individual class 1 olivine grains. Even the largest are no bigger than the megacrysts described above. It is not surprising, therefore, that they occur randomly within the upper and lower olivine-rich zones, associated with the coarser olivine phenocrysts. Because the lake appears to have become very well mixed during the eruption, it is not possible to associate the aggregates and megacrysts with a particular phase or phases, even though they may have been far from random in their occurrence in the eruption samples.

This group of dense olivine aggregates can be divided into three subcategories: (1) seven aggregates consisting dominantly of

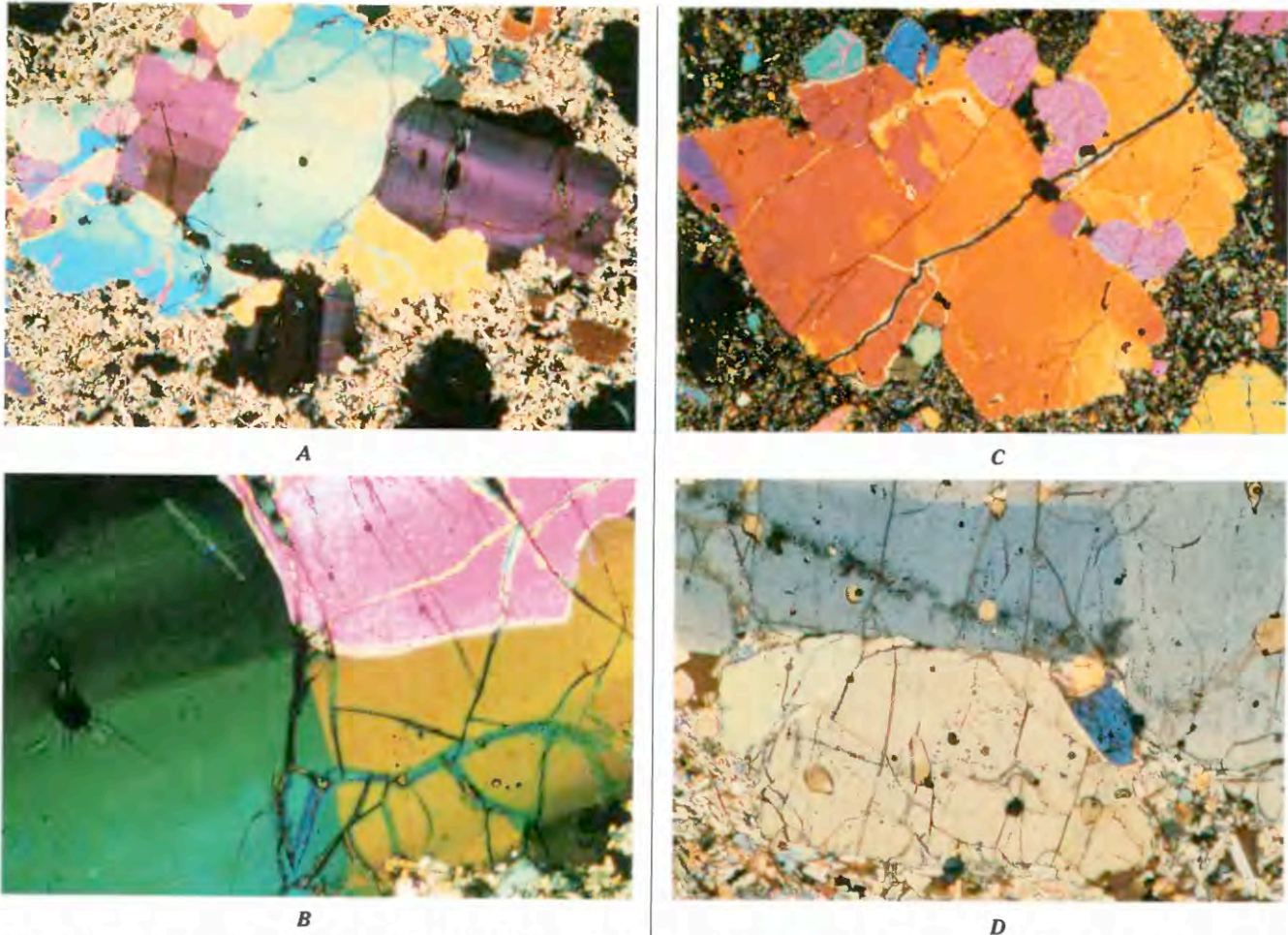


FIGURE 25.7.—Dunitic aggregates from Kilauea Iki lava lake. **A**, Aggregate of deformed olivines from KI-113, quenched from 1,090 °C–1,095 °C in 1960. All but a few of the small grains are deformed. The aggregate is 8 mm across. Crossed nicols. **B**, Close-up of a triple junction in aggregate, showing irregular grain boundaries, plus lack of 120° angles, and minimal penetration of melt from host along boundaries and at triple junction. (The black strip that intersects the triple junction is an epoxy-filled crack formed during sectioning.) Note cracks radiating from chromite inclusion in blue grain at left. Field of view 2.5 mm across. Crossed nicols. **C**, Aggregate of class 1 olivine (6 by 5 mm), from KI81-1-230.4, quenched from 1,140 °C in 1981. The large grains contain

irregular blocky subgrains, the boundaries of which are oblique to the section. Chromite (black) and smaller, strain-free olivine grains occur along the margins of the coarse olivine. Grain boundaries at triple junctions intersect at angles near 120°, and most grain boundaries are planar. Melt penetration of this aggregate is minimal, even after 22 years in the lava lake. Crossed nicols. **D**, Aggregate of class 5 olivine in KI67-2-87.5, quenched from 1,073 °C in 1967, showing swarms of inclusions. Most inclusions are very tiny. Note densest inclusion swarm trends obliquely to grain boundaries. Field of view is 1 mm across. Partly crossed nicols.

interlocking class 1 grains: (2) two clusters of class 5 grains: and (3) three aggregates containing areas of a mosaic of unstrained olivine grains.

DENSE AGGREGATES OF CLASS 1 GRAINS

This is the commonest type of dense aggregate, with seven known examples. One of these, recovered in 1960 from a depth of 6.86 m in the lake, is shown in figure 25.7A–B. It consists of anhedral grains, for the most part tightly interlocked, most containing multiple planar extinction discontinuities. Some grains contain chromite inclusions, surrounded by fractures radiating from the inclusion wall into the olivine (see fig. 25.7B). Triple junctions,

generally not intersecting at 120°, contain very small pools of glass. Two-grain boundaries can be highly irregular (fig. 25.7A–B) and are mostly unmarked by inclusions of vapor, glass, or other material. The aggregate contains a population of smaller, equant, usually unstrained grains that occur at the margins of the large grains but do not completely surround them. In the textural classifications developed for olivine-rich xenoliths from basalts and kimberlites, this and other aggregates in this group are transitional between the coarse and porphyroclastic categories of Harte (1977), or the protogranular and porphyroclastic categories of Mercier and Nicolas (1975).

The aggregate in KI-113 was quenched only nine months after the eruption ceased, so its texture may be presumed to be

relatively little affected by long-term storage in the lake. The other aggregates of class 1 grains, from 26–70 m below the surface of the lake, were cooled slowly from about 1,190 °C to the quenching temperature indicated in table 25.2 over periods of 8 to 22 years. However, the only textural change consistently observed in the latter aggregates is that the grain boundaries become more planar, and the angle of their intersections at triple junctions approach 120° (see figs. 25.5D, 25.7C). There is some tendency for greater penetration of the aggregate by melt, but, as figure 25.7C shows, this is not necessarily extensive, even after 22 years. In some of the more recently quenched samples there is a tendency for chromite to occur interstitially in the aggregate, rather than as inclusions in olivine (fig. 25.7C); but other aggregates (fig. 25.5D) have included chromite preserved.

Some aspects of the fabric of these seven aggregates are unaffected by annealing in the lake. For example, the aggregates are notably inequigranular, with the ratio of largest to smallest olivine grains present varying from 10 to 30 (see table 25.2). There is no tendency for the proportion of small grains to increase or decrease with time, nor does average grain size change in any other way as length of storage in the lake increases. Also, as in the isolated crystals, there is no discernable tendency for the kink bands or rectangular subgrains to disappear with time. The lack of internal reorganization of the large deformed grains suggests that the apparent expulsion of chromite to grain boundaries seen in some aggregates (fig. 25.7C) was accomplished during an earlier cycle of deformation and recrystallization. The present generation of subgrains, then, must have been produced in a second deformation event, the effects of which have not been eliminated by recrystallization during storage in the lake.

By decrease in number of adhering grains, these aggregates appear to grade into the dispersed class 1 olivine phenocrysts. It seems possible that all the class 1 grains and clusters found in the eruption samples and in the lake may have been disaggregated from rocks like this first group of dense, dunitic aggregates.

AGGREGATES OF CLASS 5 GRAINS

Three of the dense aggregates listed in table 25.2 contain olivine with sulfide-bearing inclusions. The two smaller ones (KI67–2–87.5 and KI79–1–203.6), consisting exclusively of class 5 grains, will be discussed here. The description below applies equally to rare smaller clusters of class 5 grains, containing 2 to 6 grains each.

A close-up view of the KI67–2–87.5 aggregate (fig. 25.7D) shows most of the features of this type. The grains are full of inclusions; some inclusions are large, of brown glass with or without opaques and vapor, but most are tiny and any glass present is pale. Included crystalline phases are chromite and sulfide. In some cases, the sulfide bleb appears to be too large to be a daughter phase, in the terminology of Roedder (1984), suggesting that such inclusions were polyphase initially, the melt already being saturated with an immiscible sulfide liquid (\pm chromite) at the time the inclusions formed. No daughter silicates have been observed. Grain shapes are

irregular, but grain boundaries are tight only locally. These aggregates all show extensive penetration of melt along grain boundaries, independent of storage time in the lake. This and the abundant inclusions give these aggregates a dirty, moth-eaten appearance in thin section.

The localization of some inclusions in the KI67–2–87.5 aggregate (fig. 25.7D) in planar arrays suggests that they formed when melt \pm sulfide, chromite, and vapor were injected into fractures in a previously existing grain or aggregate of grains. This distribution of inclusions is different from that in most class 5 grains, in which the inclusions commonly occupy either the core (as in fig. 25.5E) or a well-defined necklace (as in fig. 25.4E). The latter arrangements are more characteristic of primary inclusions, that is, inclusions incorporated during the growth of the individual olivine grain. The inclusion arrays in figure 25.7D, by contrast, appear to be secondary crack fillings (see Roedder, 1984, for a discussion of primary versus secondary inclusions). Sulfide-bearing inclusions also occur in irregular trails, swirls, and patches that cannot, from their geometry, be unequivocally designated as primary or secondary.

Class 5 grains are very rare, occurring in only 3 percent of the thin sections of drill core examined. The fact that aggregates of class 5 grains occur at all suggests that the single grains may formerly have been in aggregates, as it is highly improbable that these rare grains would coalesce into pure class-5 clusters after having been dispersed in the 1959 lava. Because of their rarity and in spite of the variation in distribution of inclusions, it seems likely that all these sulfide-bearing grains and aggregates came from a fairly limited source region.

DENSE AGGREGATES CONTAINING POLYGONAL MOSAICS OF OLIVINE

Three of the dunitic aggregates described in table 25.2 consist partly or entirely of a mosaic of equigranular polygonal olivine. Two of these (in KI79–5–171.4 and KI81–1–181.5) are the largest known aggregates in the lake. Each of the three is slightly different in character, having a different range of grain sizes in the mosaic areas, as follows:

KI67–2–87.9	-----	0.6–2.5 mm
KI79–5–171.4	-----	0.4–1.0 mm
KI81–1–181.5	-----	0.05–0.2 mm

The grain size of the mosaics is independent of storage time in the lake, as the coarsest was quenched in 1967 and the finest grained in 1981. Mosaic textures similar to those shown in figure 25.8A–C have been produced experimentally by thermal annealing (Mercier, 1979, p. 200, fig. 2d). None of the grains in the mosaics show any sign of strain, suggesting that they were not produced by recrystallization during steady-state deformation of the sort studied by Ross and others (1980). The lack of correlation between mosaic grain size and time of storage in the lake suggests that none of these mosaics was produced during post-eruptive annealing in the lake.

The smallest and simplest of these three aggregates (fig. 25.8C) consists of strain-free grains with curvilinear boundaries and limited size range. This texture corresponds to the equant gran-

TABLE 25.2.—Data on olivine aggregates and megacrysts found in Kilauea Iki lava lake

Sample	Depth of sample (m)	Date drilled (mo/d/yr)	Quenching temperature (°C)	Location in lake	Size of aggregate in section (mm)	Crystal size range		Size ratio (largest/smallest)	Dominant crystal class
						Largest (mm)	Smallest (mm)		
Olivine Aggregates									
KI-113	6.86	8/24/60	1090-1095	center	8 x 5	4	0.2	20	1
KI67-2-87.5	26.67	6/14/67	1073	north edge	7 x 5	6	0.5	12	5
KI67-2-87.9	26.79	7/6/67	1090	north edge	(a) ¹ 12 x 7 (b) 9 x 3	8 2.5	0.8 0.6	10 4	1 Polygonal mosaic
KI79-5-171.4	52.24	2/1/79	950-980	north edge	¹ 14 x 10	7	0.4	28	Polygonal mosaic
KI81-1-181.5	55.32	4/10/81	1010-1030	center	^{1,2} 16 x 4	2	< 0.1	> 20	Polygonal mosaic
KI79-1-189.0	57.61	12/21/78	1130-1135	center	(a) ¹ 8 x 6 (b) ¹ 6 x 6	6 6	0.4 0.6	15 10	1 1
KI79-6-190.3	58.00	2/14/79	1130-1135	between center and north edge	5 x 4	5	0.5	10	1
KI79-1-203.6	62.06	12/21/78	1140	center	3 x 2	2	0.3	7	5
KI81-1-224.4	68.40	4/13/81	1140	center	10 x 5	8	0.5	16	1
KI81-1-230.4	70.23	4/13/81	1140	center	6 x 5	6	0.2	30	1
Megacrysts									
KI76-2-20.5	6.25	8/30/76	~100	center	¹ 20 x 10	single crystal		-	-
KI81-1-238	72.54	4/14/81	1135-1140	center	¹ 20 x 10	single crystal		-	-

¹ Cut by edge of section. Area given is that within the section.

² Area of aggregate on drill core surface 16 mm x 10 mm. The section was cut perpendicular to the core surface.

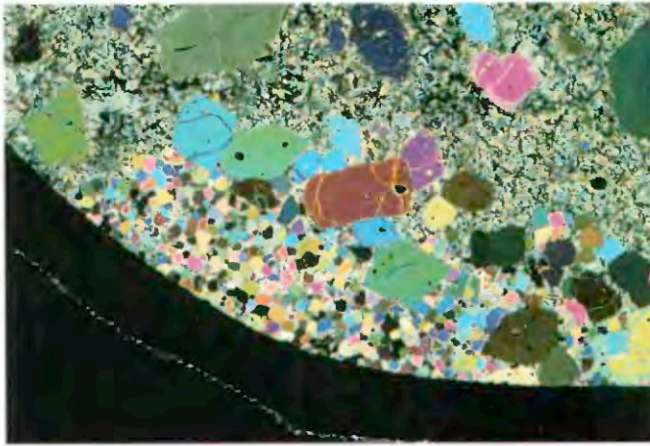
uloblastic category of Harte (1977) or the mosaic equigranular category of Mercier and Nicolas (1975, fig. 6b, p. 464), a texture attributed to lengthy annealing at high temperatures. The olivines in this inclusion contain abundant healed discoid fractures similar to textures in olivines from San Carlos and elsewhere, which have been interpreted (Wanamaker and Evans, 1985) as produced by decrepitation of fluid inclusions during rapid decompression. Similar healed fractures occur in inclusions KI67-2-87.5 and KI79-1-189.0(a), but are not as common in these aggregates as in figure 25.8C.

The KI81-1-181.5 aggregate is more complex, in that it contains, in addition to the fine-grained mosaic shown in figure 25.8B, a population of coarser, more euhedral crystals, commonly containing a necklace of inclusions, some with sparse, tiny sulfide blebs. The coarser grains probably represent a second stage of grain coarsening, with the larger crystals having grown at the expense of smaller ones. The necklace of inclusions would correspond to impurities along former boundaries of the grains, swept up as the olivine grains grew outward. For the following reasons, this interpretation is preferred to a model in which the coarser grains would be considered to be later cumulates that attached themselves to a preexisting fine-grained substrate: First, some of the coarse grains occur within the mosaic, not at its edge. Second, the grains are very tightly intergrown and randomly oriented (unlike the open cumulate

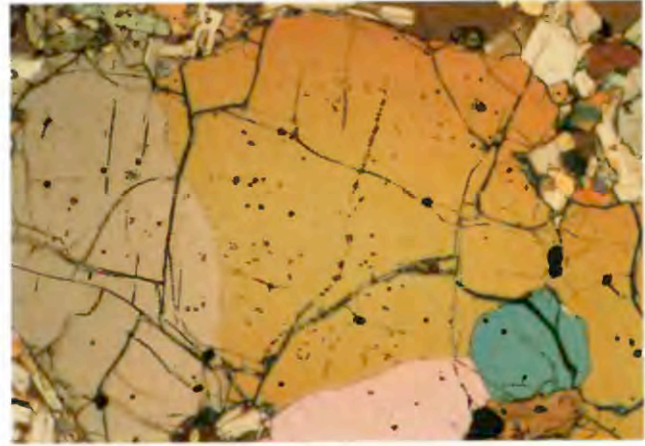
aggregates shown in fig. 25.6A-B). Third, the small mosaic grains contain very tiny inclusions similar in character to those in the coarser grains, suggesting that the coarse grains grew by incorporating this mosaic and its grain-boundary phases. Clearly the second-stage coarsening did not take place in the lava lake; the mosaic at the left end of the aggregate (fig. 25.8D) is in direct contact with the host and shows no coarsening whatever. Therefore, both stages predate incorporation in the present host.

The third of these aggregates, from sample KI79-5-171.4 (fig. 25.8D), is the most heterogeneous and also the most enigmatic. It contains areas where deformed class 1 grains are partly enclosed by strain-free polygonal grains, but elsewhere it contains euhedral, class-2-like grains. This aggregate also shows more extensive penetration by melt (now groundmass crystals) than any other aggregate. Of all the aggregates in table 25.2, this one appears to have the most complex history.

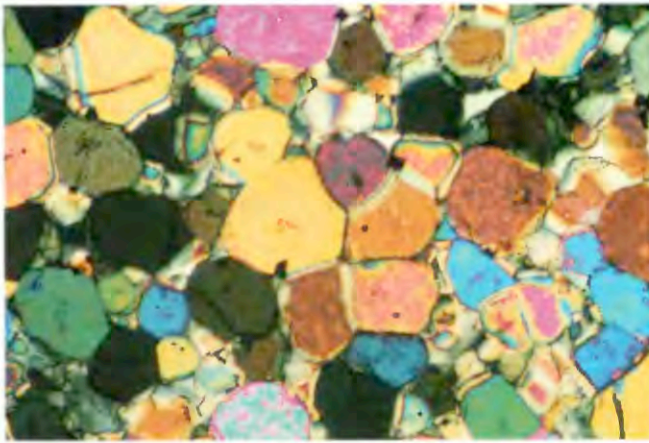
In contrast to the other two groups of aggregates, which correspond to one or another of the olivine classes described above, the mosaic grains do not occur as a recognizable separate class of dispersed grains. It is possible that some of the smallest class 1 and some class 3 grains might be former polygonal mosaic, but this seems unlikely: there are very few such grains in the eruption pumice. A more likely explanation is that strongly annealed dunites are simply rarer than the mildly deformed ones.



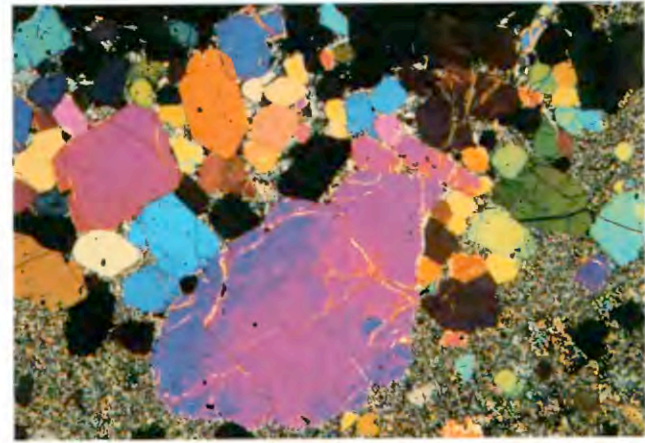
A



C



B



D

FIGURE 25.8.—Dunitic aggregates found in Kilauea Iki lava lake. **A**, Olivine aggregate and host in KI181-1-181.5, quenched from 1,010–1,030 °C in 1981. Field of view is 1 cm across. The aggregate consists of areas of fine-grained polygonal mosaic of olivine, with coarser, more euhedral olivine present along the edge or (lower right) within the mosaic. At the left end of the aggregate, the mosaic is in direct contact with the groundmass of the host. Crossed nicols. **B**, Close-up of polygonal mosaic in aggregate in KI181-1-181.5. Field of view 1 mm across. Most grains are olivine. Most of the olivine grains contain a central swarm of tiny inclusions (see yellow grains in center). Chromite grains (opaque) occur at margins of olivine. Minor interstitial plagioclase and augite are present locally. Crossed nicols. **C**, Close up of the smaller olivine aggregate from KI67-2-87.9,

quenched from 1,090 °C in 1967. Grain boundaries intersect at angles near 120° at triple junctions, but are otherwise curvilinear, so that grain shapes are irregular. The color variation seen in the tan olivine grains reflects zoning toward the host; it follows the outline of the aggregate, not of individual grains. Black grains within the aggregate are chromite. Fuzzy inclusions are healed discoid fractures containing asterisk-like inclusions of brown glass and chromite. Field of view is 4 mm across. Nicols partly crossed. **D**, Olivine aggregate (10 by 14 mm) in sample KI179-5-171.4, quenched from 950–980 °C in 1979. This aggregate has been extensively penetrated by melt, now visible as interstitial groundmass-size crystals. It contains local areas of polygonal olivine, surrounding coarser deformed olivine (the green grains on right side), and areas of randomly oriented euhedral olivine (center and left). Crossed nicols.

In summary, then, rare dunitic aggregates have been found in Kilauea Iki lava lake. The textures of the various aggregates, which record multiple deformation events, multiple annealing events, and (or) rapid decompression, match those observed in ultramafic xenoliths of mantle origin. The fact that the history recorded in these aggregates appears to predate entirely their incorporation in the 1959 lava implies that all aggregates are xenolithic. To the extent that class 1 and class 5 olivine grains in the 1959 lava are derived by disaggregation from similar preexisting dunite, crystals in those classes may likewise be considered xenocrystic.

OLIVINE PHENOCRYSTS AND DUNITIC AGGREGATES IN OTHER HAWAIIAN ROCKS

Olivine is virtually ubiquitous as a phenocryst phase in Hawaiian tholeiites and mafic alkalic rocks. With the petrographic description of the phenocrysts, megacrysts, and dense aggregates found in the Kilauea Iki lava in hand, it is now appropriate to review the information available on the petrography of olivine from other Kilauea lava and from those of other Hawaiian volcanoes.

No comparably detailed petrographic work on Kilauea

olivines has been done previously. Even studies focused on the picritic lava of Kilauea (Macdonald, 1944; Muir and Tilley, 1957; Murata and Richter, 1966a, 1966b) have not mentioned the occurrence of kink-banded olivine, for example. Therefore I have re-examined all of the thin sections of subaerial Kilauea basalt available to me, with the present classification scheme in mind. The available sections included samples of the historical eruptions described in Wright (1971), including the 1920 eruption, the relatively magnesian 1921 summit eruption, and the 1840 east-rift picrite. In addition, samples of the 1977, April 1982, and September 1982 eruptions, and samples of phases 1–8 of the ongoing (as of January 1986) Puu Oo eruption have been examined. The earlier samples were available only as covered thin sections; for the 1977–1983 samples, polished sections were available for examination.

One good example of a kink-banded olivine phenocryst was found in this search, in TLW 67-1g, the most magnesian lava of the 1920 southwest-rift eruption (Wright, 1971). No other class 1 or probable class 5 olivine has been observed in any of them. The olivine phenocrysts present all fall in class 2 of the present classification system, being either euhedral or skeletal. Skeletal grains are much more common, proportionately, than they are in Kilauea Iki samples. Resorbed grains, though present (in some Puu Oo samples, for instance), are rare.

The olivine-rich precaldra intrusive rocks exposed in Kilauea's caldera wall, including the Uwekahuna laccolith, were also examined, with the thought that they might represent samples of olivine-rich sludge from the bottom of Kilauea's summit reservoir. The olivine phenocrysts in these intrusives are uniform in grain size (1–5 mm long) in contrast to the more variable olivine in Kilauea Iki (see fig. 25.3). Planar extinction discontinuities were observed in very few grains. These grains are small, and the bands very faint. In about one-half the cases, the discontinuities exist only at the margin of the grain and are absent from the interior. No such grains have been observed in the 1959 lava, and it is not clear whether these marginal extinction discontinuities are deformation or growth features.

Examination of the submarine east-rift lava described by Moore (1965) turned up deformed olivine in two samples, No. 1742, from 1,400 m below sea level, and No. 1706, from 5,000 m below sea level. Another dredged sample of Kilauea east-rift lava, shown to me by M.O. Garcia (University of Hawaii) also contains good examples of blocky, deformed olivine crystals, strikingly similar to those in the 1959 lava.

In addition to these instances of kink-banded olivine in Kilauea tholeiite, such olivine has been reported from tholeiite of Hualalai, dredged from 2 km below sea level (Clague, 1982) and in one Haleakala tholeiite in the suite studied by Chen and Frey (1983) (C.-Y. Chen, written commun., 1984). Thus, the kink-banded olivine in the 1959 Kilauea tholeiite are not unique. However, they appear to be virtually absent from other subaerial Kilauea eruptions.

Dunitic aggregates containing deformed olivine and (or) mosaics of unstrained grains occur very widely in alkalic rocks in Hawaii. They have been described from Hualalai (Kirby and

Green, 1980; Jackson and others, 1981), from the Honolulu Volcanics (formerly the Honolulu Volcanic Series; Jackson and Wright, 1970; Sen, 1983), and from Loihi Seamount (Moore and others, 1982; Roedder, 1983). Other reports of similar materials in Hawaiian tholeiite are lacking, however. Jackson (1968), in his very extensive survey of coarse-grained xenoliths in Hawaiian rocks, stated that all coarse-grained xenoliths he had found in tholeiitic lavas were cumulates, and that "none of the minerals is strained or deformed" (Jackson, 1968, p. 142). He further presented data showing that pure olivine rocks, containing no other cumulus or interstitial phases, were very rare in Hawaiian tholeiite. The deformed dunitic aggregates found in Kilauea Iki appear to be the first such material recognized in any Hawaiian tholeiite.

OLIVINE AND GLASS COMPOSITIONS: ERUPTION PUMICE

This section presents compositional data on olivine and glass in the eruption samples. Of particular interest are (1) variations in composition and zoning of the olivine phenocrysts as a function of petrographic class and of time, (2) variations in average glass composition with time, and (3) more detailed data on the glasses immediately adjacent to olivine phenocrysts in the eruption pumice. As will become evident, these rapidly quenched samples preserve a significant amount of internal disequilibrium, as might be expected in an eruption long-recognized as involving magma mixing (Wright, 1973).

Analyses of representative olivine grains are presented in table 25.3. These analyses cover the range of phenocryst composition observed. The forsterite contents shown are reproducible to ± 0.1 percent, MnO ± 0.02 percent, CaO to ± 0.03 percent absolute. NiO is more variable, reproducible to perhaps ± 0.05 percent absolute. The intragrain chemical variation (see table 25.3, columns 1 and 2, for example) is modest, but it exceeds the analytical uncertainty and is generally systematic, with the cores being uniform and all variation (zoning) confined to the rims. There are a few grains, especially in the later samples, where forsterite content varies more irregularly, but the total range of intragrain variation in these grains is ≤ 0.8 mol percent Fo. Therefore, it seems justifiable to document, and to interpret, the zoning patterns of most of these olivines.

Table 25.4 includes average glass compositions for the fifteen eruption samples studied. These include only glass analyses taken some distance (>1 mm) away from the olivine phenocrysts. All of the glass compositions are olivine-controlled (Powers, 1955; Wright, 1971); that is, they are related to each other chiefly by addition or removal of olivine (\pm chromite), the only phenocryst phase present. Hence, the most variable component is MgO, which ranges from 6.35 to 10.03 weight percent and is reproducible to ± 0.10 percent. Other oxides are less variable: total iron as FeO only varies from 11.00 to 11.65 percent, for example. As documented in Helz and Thornber (in press), the MgO content of Kilauea glass in equilibrium with olivine varies linearly with temperature and appears to be a usable geothermometer. The quenching

temperature assigned each glass in table 25.4 is based on this calibration.

OLIVINE PHENOCRYST COMPOSITION VERSUS PETROGRAPHIC CLASS

Olivine compositional data as a function of the petrographic classes established above are presented in figures 25.9A–B and 25.10. Figure 25.9A shows histograms of the forsterite content of the cores of all the olivine phenocrysts analyzed to date. Each symbol corresponds to one analyzed point. For grains showing <0.5 percent variation in forsterite, all points are plotted. Most such grains are strongly resorbed (class 3 or 1) or fragmental (class 4) and may not have any real rims preserved on them.

The most important feature of figure 25.9A is that there is extensive overlap in core compositions between the euhedral class 2 olivine and the less regularly shaped, kink-banded and (or) sulfide-bearing olivine in classes 1 and 5. Class 1 and 5 cores extend to higher forsterite contents (88.7 percent), and class 2 cores to lower forsterite contents (85.0 percent), but the bulk of both subsets fall between 85 and 88 percent Fo. The class 3 and 4 grains are not distinctive, with most having 86.5–87.7 percent Fo. It should be noted that the composition of olivine from phase 1 (which made up most of the lake; see fig. 25.2) is no different from that of olivine in the later phases, except that the most iron-rich class 2 grains are absent.

TABLE 25.3.—Composition of selected olivine grains from the 1959 eruption pumice, showing extremes of composition and zoning
[Oxide contents in weight percent]

Sample	Iki-22		Iki-9		Iki-24 core
	core	rim	core	rim	
Olivine class	1	1	2	2	1
Points in analysis	5	4	2	4	3
SiO ₂ -----	39.44	39.90	40.09	38.95	40.22
TiO ₂ -----	.01	.01	.05	.04	.00
Al ₂ O ₃ -----	.03	.02	.00	.02	.00
Cr ₂ O ₃ -----	.02	.00	.04	.02	.01
FeO-----	14.22	12.09	12.26	18.16	11.03
NiO-----	.10	.19	.15	.01	.17
MnO-----	.20	.17	.12	.20	.17
MgO-----	45.86	47.76	47.38	42.37	47.87
CaO-----	.24	.20	.24	.32	.25
Na ₂ O-----	.00	.00	.00	.02	.02
Total-----	100.12	100.34	100.33	100.11	99.74
percent					
Mol% Fo	85.2	87.6	87.3	80.6	88.6
Comments	Reverse zoning		Extreme normal zoning		Most magnesian

Most of the olivine phenocrysts in the eruption samples are zoned, and figure 25.9B summarizes the available data on zoning patterns for the same population of grains whose core compositions were given in figure 25.9A. Most grains vary over a range of 3 percent Fo or less, the zoning generally being confined to the outermost 10–30 μm of the crystal. Only two small class 2 grains are more strongly zoned, showing as much as an 8 percent decrease in Fo from core to rim. The class 3 and 4 grains are essentially unzoned.

Three features of figure 25.9B are particularly noteworthy. First, normally zoned and reversely zoned grains are almost equally abundant. Second, there is little difference between the euhedral class 2 grains and the class 1 and 5 grains in this respect. If anything, reverse zoning is more frequent in the class 2 population. Lastly, the olivine phenocrysts analyzed so far from phase 1 samples are mostly either reversely zoned or unzoned. Normally zoned phenocrysts do not become common until phase 2.

The variation in NiO content of olivine cores for this same population of grains is shown in figure 25.10. NiO content was of particular interest because potentially it might allow one to distinguish between cognate and xenocrystic (peridotite-derived) olivine, or perhaps between olivine that coexisted with sulfide and olivine that did not. As can be seen in figure 25.10, however, the various populations appear not to have distinctive NiO contents. The few class 5 sulfide-bearing grains in the eruption pumice tend to fall below the median NiO content for the class 1 + 5 grains overall, but even here the difference is not very marked. (It should be noted that all the sulfides in the class 5 grains in the eruption samples are tiny, hence do not unequivocally predate entrapment and therefore do not prove that the basaltic melt from which the olivine in fig. 25.10 grew was sulfide-saturated.) From the analyses in table 25.3 one might suppose that there was a positive correlation between NiO and forsterite contents, but when the entire data set is considered there is no such correlation. The NiO contents observed here (0.10–0.30 percent) are the same as reported by other workers for Kilauea basalt (Häkli and Wright, 1969; Bence and others, 1981) and other mafic rocks (Fleet and others 1977; Fleet and MacRae, 1983).

It is evident from figures 25.9A–B and 25.10 that the various petrographic classes of olivine described earlier are not distinct with respect to Fo content or NiO content or style of zoning. They are not distinguishable on the basis of MnO or CaO contents either. This suggests that the olivine grains formed under some continuous range of conditions and that none of the classes can be singled out on the basis of composition as being xenocrystic to their host.

The results presented above are slightly at variance with those of some earlier workers. Richter and Murata (1966) reported that large blocky olivine phenocrysts were magnesian (Fo_{87–88}) and small euhedral olivine crystals more iron-rich (Fo₈₂). Certainly individual crystals can be found with these characteristics, but the composition ranges of the two populations overlap almost completely. Even the microphenocrysts (not shown in figs. 25.9A–B, 25.10) range from Fo₈₇ to Fo₇₄. Thus, the various olivine groups cannot be considered to be successive generations of crystals grown

TABLE 25.4.—Composition of glass away from olivine phenocrysts in selected samples of the 1959 Kilauea eruption pumice
[Oxide contents in weight percent; total iron reported as FeO]

	1	2	3	4	5	6	7	8	9	10	11	12	13	14	15
Sample No.	Iki-1	Iki-58	Iki-22	Iki-44	Iki-7	Iki-11	Iki-9	Iki-13	Iki-14	Iki-20	Iki-21	Iki-24	Iki-26	Iki-32	Iki-33
Date (mo/d) sample collected	11/14	11/15	11/18	11/20	11/21	11/26	11/28	12/5	12/6	12/8	12/11	12/13	12/14	12/17	12/19
Phase of eruption	1	1	1	1	1	2	3	4	5	7	8	9	10	15	16
SiO ₂	49.91	50.23	49.18	49.46	49.62	49.32	50.46	49.84	49.43	49.81	49.76	49.88	49.26	49.65	49.63
TiO ₂	2.96	2.91	2.49	2.66	2.64	2.64	2.82	2.62	2.60	2.60	2.63	2.68	2.67	2.63	2.63
Al ₂ O ₃	13.99	13.98	12.10	12.82	12.88	12.69	13.51	12.74	12.73	13.02	12.85	13.19	12.98	12.93	13.03
Cr ₂ O ₃	.01	.00	.08	.07	.05	.06	.01	.07	.06	.04	.07	.07	.06	.04	.06
FeO	11.40	11.65	11.33	11.27	11.25	11.15	11.00	11.14	11.27	11.28	11.21	11.04	10.92	11.08	11.22
MnO	.13	.14	.13	.14	.13	.12	.14	.13	.13	.13	.13	.13	.13	.13	.12
MgO	6.35	6.46	10.03	8.55	8.60	8.48	6.93	9.04	9.49	8.21	9.09	8.61	8.67	8.73	8.70
CaO	11.25	11.50	11.17	11.25	11.33	11.39	11.56	11.39	11.38	11.33	11.41	11.51	11.51	11.55	11.67
Na ₂ O	2.67	2.62	2.33	2.53	2.46	2.51	2.48	2.36	2.29	2.32	2.39	2.17	2.46	2.45	2.28
K ₂ O	.62	.60	.52	.54	.56	.56	.58	.55	.58	.54	.55	.58	.52	.54	.60
P ₂ O ₅	.28	.26	.22	.26	.25	.27	.31	.23	.21	.27	.26	.24	.24	.23	.24
Total	99.57	100.35	99.58	99.55	99.77	99.19	99.80	100.11	100.17	99.51	100.35	100.10	99.42	99.96	100.18
Points in average	8	14	6	6	7	4	6	9	5	5	7	4	6	5	4
Quenching temperature (°C)	1142	1144	1216	1187	1188	1185	1154	1196	1205	1181	1197	1188	1189	1191	1190

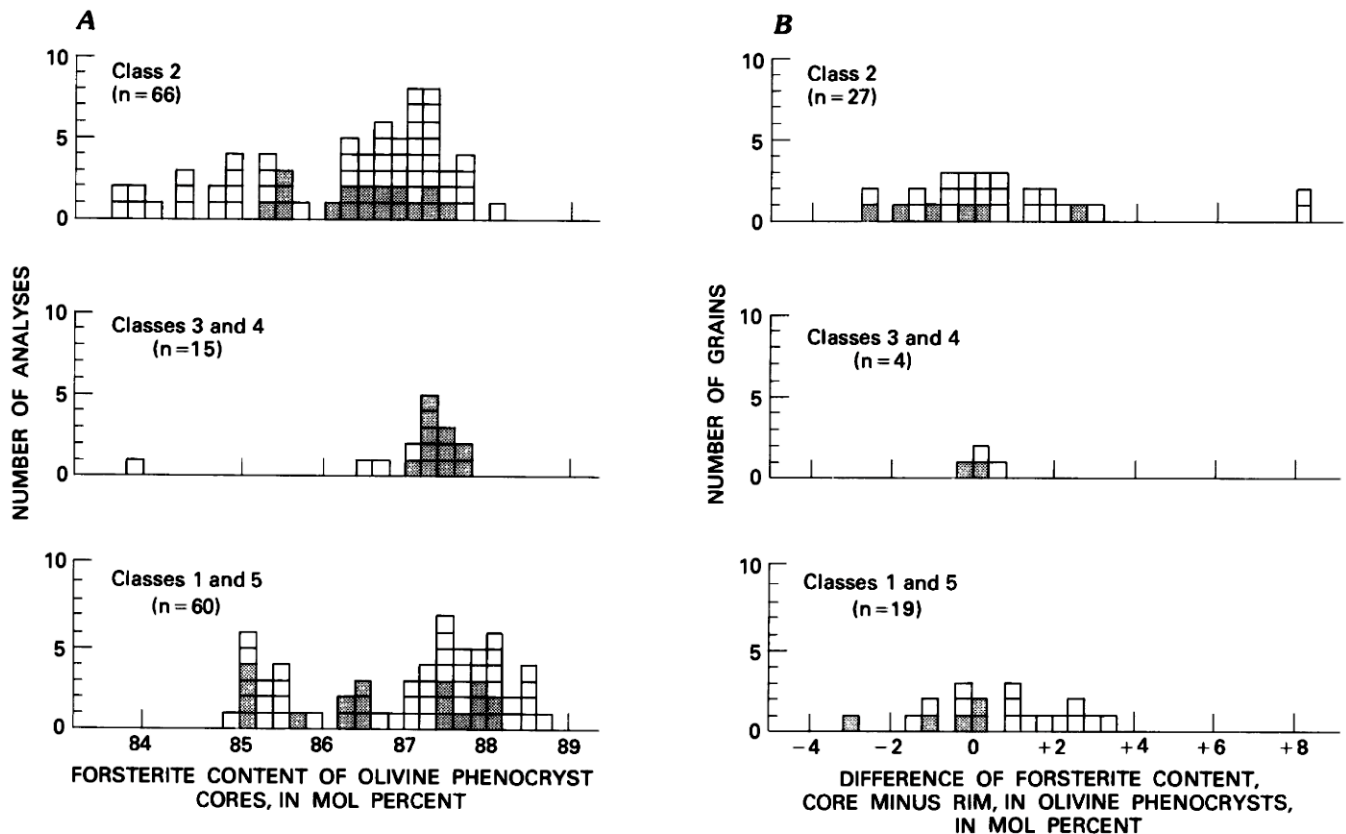


FIGURE 25.9.—Compositional data for olivine phenocrysts from the 1959 Kilauea eruption. Shaded squares, olivine from phase 1; open squares, olivine from later phases. **A**, Frequency distribution of forsterite content of the cores of olivine phenocrysts in eruption samples. Each square represents one analyzed point. **B**,

Frequency distribution of different types of Mg-Fe zoning observed in olivine phenocrysts in eruption samples, for the same olivine population as in fig. 25.9A. Each square represents one grain. Negative abscissa values indicate reverse zoning.

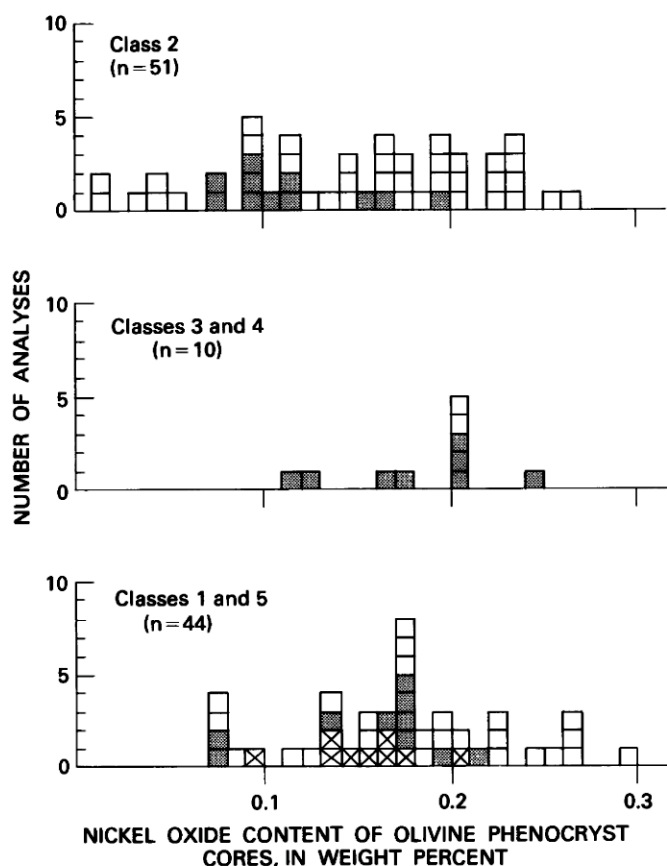


FIGURE 25.10.—NiO content of the cores of olivine phenocrysts in the 1959 Kilauea eruption samples, for the same population of olivine grains as in fig. 25.9. Each square represents one analyzed point. There are fewer points in this figure than in figure 25.9 because Ni was not always analyzed for. Shaded squares, phase 1 olivine; squares with x, class 5 olivine, from phases 2–16; open squares, other olivine from phases 2–16. The calculated limit of detection of NiO is 0.08 weight percent.

from a single batch of magma.

The data in figure 25.9B, showing that most olivine phenocrysts are zoned, are superficially in conflict with Leeman and Scheidegger's (1977) statement that the olivine in the 1959 eruption is not zoned. This is a question of semantics, however: Leeman and Scheidegger chose to regard any grain that varied by less than 5 percent Fo as unzoned, and it is true that strongly zoned grains are rare in the 1959 lava.

OLIVINE PHENOCRYST COMPOSITIONS VERSUS TIME

It is evident from figure 25.9A–B that olivine compositions and zoning patterns vary slightly from phase to phase of the eruption. These variations from sample to sample are shown in figure 25.11. Note that in this figure, in contrast to figures 25.9A and 25.10, symbols correspond to more than one analyzed point. For example, in sample Iki–11, three grains have been analyzed,

one each from classes 1, 2, and 5. There are six analyzed core points and three rim points on the class 5 grain, but some of the core points fall on top of each other, so are not visible as separate points in figure 25.11. Average MgO content of the glass in each sample (see table 25.4) is plotted below the olivine data. The range of MgO content shown is that observed in glass more than 1 mm away from any olivine phenocryst. The fields in figure 25.11 outline the range of core compositions for the two groups of olivine.

As noted above, olivine is sparse in the cool (1,140–1,145 °C), early phase 1 samples. The olivine grains are small and euhedral, but with variable zoning. Iki–22, the first of the olivine-rich samples, has a much more magnesian glass with a quenching temperature of 1,217 °C (see table 25.4) and a phenocryst population of large, reversely zoned olivine crystals. Previous workers (Leeman and Scheidegger¹ 1977; Ford and others, 1983; Harris and Anderson, 1983) have noted that the cores of these olivine phenocrysts would be in equilibrium with the glass in the sample at about 1,250 °C. None has reported the existence of the more magnesian rims, however.

In contrast to Iki–22, Iki–44 has only fairly magnesian olivine grains in it, all virtually unzoned. The glass in this sample was quenched from a lower temperature (1,189 °C) than that in Iki–22. The glass in Iki–7 is similar to that in Iki–44 but it includes, besides magnesian, unzoned olivines like those in Iki–44, reversely zoned euhedral olivines, some of which are shown in figure 25.4C. Thus, in phase 1 we see a large range in glass composition and a significant range in olivine composition (Fo₈₈ to Fo_{84.5}). However, there is no correlation between glass composition and olivine core composition, olivine rim composition, or the style of zoning, if any. As noted above, all large zoned olivine grains in phase 1 are reversely zoned.

Phase 2 (Iki–11) contains the first coarse, normally zoned olivine, in addition to reversely zoned crystals. The crystals do not converge on a common rim composition, however: the class 1 crystals range from Fo_{87.8} (core) to Fo₈₅ (rim), whereas the class 2 crystals go from Fo₈₅ (core) to Fo_{87.4} (rim). Further evidence of internal disequilibrium is the observation that the glass in this sample is appreciably more heterogeneous than that in any individual phase 1 sample, with MgO ranging from 8.07 to 8.60 percent, for glasses well away from olivine.

Phase 3 (Iki–9), like Iki–58 from phase 1, though olivine-poor, does not contain a uniform olivine population. Only two small class 2 olivines occur in the thin section, but they show very different zoning patterns: one ranges from Fo_{87.4} to Fo_{79.3} and is euhedral at the edges; the other varies from Fo_{84.9} to Fo_{83.1} and is resorbed at the edges. The glass in this sample was quenched from a lower temperature (1,154 °C) and is more differentiated than that in any but the earliest phase 1 samples.

Phase 4 glass (Iki–13) is again more magnesian, with a quenching temperature of 1,196 °C, and the glass is more hetero-

¹Leeman and Scheidegger (1977) refer to Iki–22 as KI–7 and to what is probably Iki–7 as KI–22. This is a numbering mixup: Iki–22 has a unique high-MgO glass not found in any other phase 1 pumice. Ford and others (1983), using Leeman and Scheidegger's data, reproduce the same numbering error.

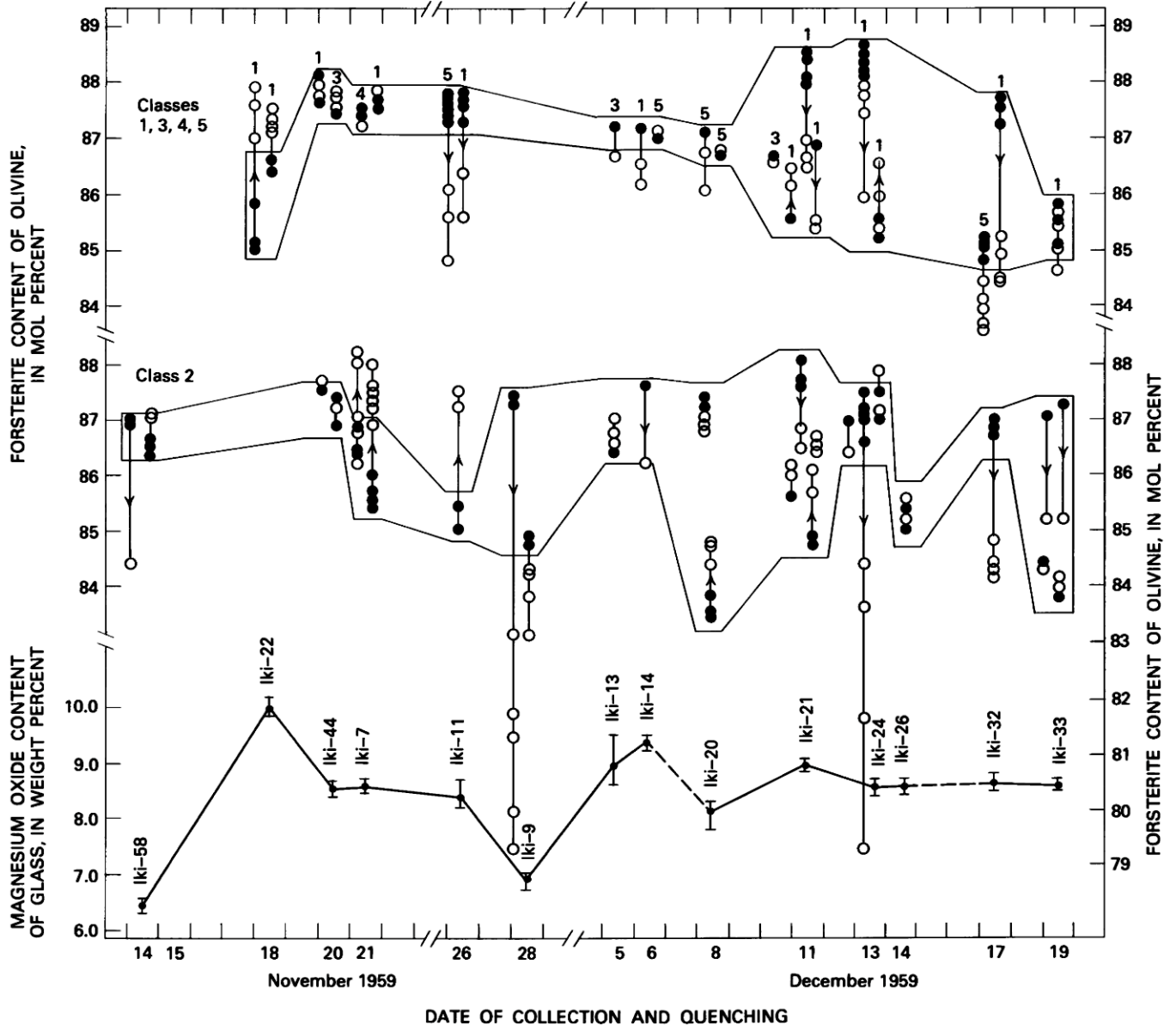


FIGURE 25.11.—Composition of olivine phenocrysts (mol percent Fo) and of glass (weight percent MgO) in samples from the 1959 eruption of Kilauea, plotted against the dates of eruption and quenching. For olivine, each symbol includes all analyzed points on a given grain having the same composition, rounded to 0.1 percent Fo. All data from a given grain are connected by a line. Solid circles, analyzed points from the cores of grains; open circles, points around the rims of the

same grains. Grains in classes 1, 3, 4 and 5 are individually labeled. Arrows pointing toward rim compositions emphasize the direction of zoning. For glass, the small dots give the average MgO content of glass, from table 25.4, whereas the bar indicates the total range of MgO content observed, for glass more than 1 mm away from olivine.

geneous than any other sample, with MgO varying from 8.70 to 9.48 percent. Phase 5 (Iki-14) contains a still hotter (1,205 °C) but more uniform glass, with 9.32 to 9.55 percent MgO. In both samples, olivine phenocrysts are weakly zoned, in both normal and reverse senses, and are consistently magnesian ($Fo_{87.5}$ to $Fo_{86.0}$).

Phase 6 is not represented here. Phase 7 (Iki-20) is, again, a cooler phase (1,181 °C), though not as differentiated or olivine-poor

as phase 3. The olivine population within the section is more diverse than ever: Both normally and reversely zoned grains are present, and the class 2 olivine exhibits a wide range of core compositions ($Fo_{87.5}$ to $Fo_{83.4}$). For the first time, however, the rim compositions of the different grains converge toward a common composition, as though they had been trying to equilibrate, either with each other or with a common melt.

Phase 8 (Iki-21) is hotter again (1,197 °C) and very olivine-rich, with a very heterogeneous olivine population. As in phase 7, the rims of the various class 2 grains appear to be converging on a common composition. This sample contains the most magnesian ($Fo_{88.1}$) class 2 olivine found.

Phase 9 (Iki-24, see fig. 25.3) contains a slightly cooler (1,188 °C) glass. Like Iki-21, it contains a very varied group of olivine crystals, with the class 1 grains converging on a common rim composition. It also contains the only strongly zoned grain ($Fo_{87.5}$ to $Fo_{79.3}$) found since phase 3, and the most magnesian olivine ($Fo_{88.7}$) in the whole analyzed population shown in figure 25.11.

From phase 10 through phase 16 (samples Iki-26, Iki-32, and Iki-33), glass composition is constant, implying uniform quenching temperatures of 1,188–1,190 °C. The glass is quite homogeneous, away from olivine, within each section. The olivine grains are either normally zoned or unzoned; none shows pronounced reverse zoning. Also, although core composition remains quite varied, olivine rim compositions are consistently more iron-rich ($Fo_{85.5}$ to $Fo_{83.5}$) than in all previous phases but phase 3. This trend toward simpler, better equilibrated olivine compositional variations begins earlier than the simplification in the petrographic variants, which is confined to phases 16 and 17 (see table 25.1).

COMPOSITION OF GLASS ADJACENT TO OLIVINE

The glass compositions presented in table 25.4 and discussed above are those found more than 1 mm away from any olivine phenocryst. Glass closer to olivine grains is more variable in composition, in ways that cannot be explained as the result of quench overgrowths on olivine. This section presents data on selected pairs of olivine rim and adjacent glass that illustrate both this greater variation in the glass and its apparent correlation with the condition (euhedral or resorbed) of the adjacent olivine rim.

The olivine rim compositions (shown in fig. 25.11) were taken on points within 10 μm (and usually within 3–5 μm) of the contact of the olivine with the glass. The adjacent glass analyses are taken at distances of 20–30 μm away from the contact. Most of the rim points shown in figure 25.11 have a corresponding analysis of adjacent glass. From this data set, figure 25.12 includes data on only three samples: two phase 1 samples (Iki-22, Iki-44) and the latest analyzed sample (Iki-33, from phase 16).

In Iki-22, glass adjacent to the large reversely zoned phenocrysts is less magnesian than glass elsewhere in the section. Around the edge of each crystal, glass adjacent to euhedral corners and faces is more magnesian than glass adjacent to resorbed edges. Some of this resorption is very local (fig. 25.13). It is possible that all the adjacent glass has been depleted in MgO by growth of olivine during quenching, but the variation within the adjacent glass cannot be so explained; the analyzed points are all equally far from olivine.

The glass in Iki-44 is less magnesian and the olivine more magnesian than Iki-22, as noted above. Here we see data from four different grains, two in a cluster and two isolated phenocrysts. Three of these grains have adjacent glass analyses with MgO

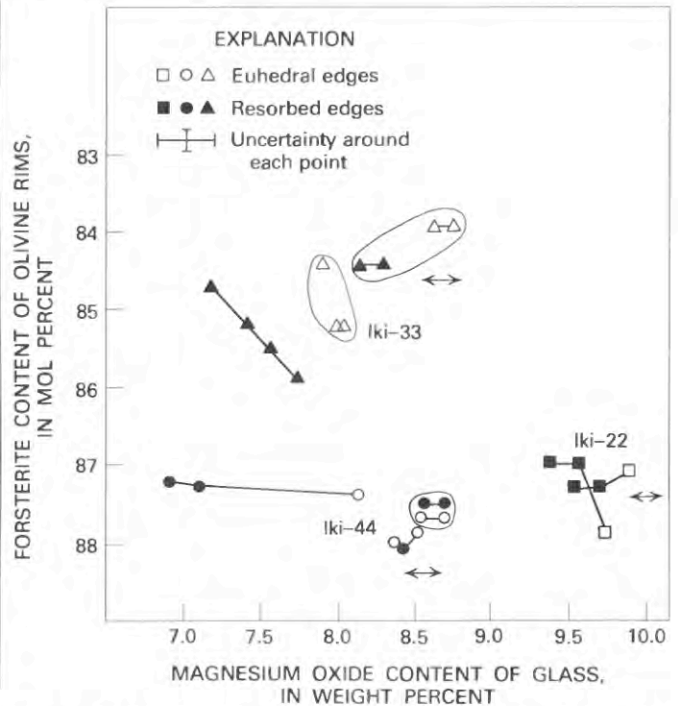


FIGURE 25.12.—Composition of rims of olivine phenocrysts (mol percent Fo) plotted against the MgO content (weight percent) of glass adjacent to the olivine rim, for three samples from the 1959 Kilauea eruption. Squares, data from Iki-22; circles, data from Iki-44; triangles, data from Iki-32. In this figure, points connected by a line are from around the periphery of a single grain. Data within a circle represents points on two or more different grains from a cluster of olivine grains. The double-ended arrow shows the range of MgO in glass more than 1 mm from olivine for each of the samples. The uncertainty in Fo and in MgO is ± 0.1 percent.



FIGURE 25.13.—Large olivine grain from Iki-22, showing euhedral form locally modified by resorption. Cusped edges like this are also visible in figure 25.4E. Field of view 2 mm across. Crossed nicols.

contents close to the average MgO content of the distant glass; these glasses appear to be unaffected by any quench overgrowths on olivine. The fourth grain is surrounded by a sheath of variable, but less magnesian glass, some of which is grossly different in composition from glass elsewhere in the thin section. As in Iki-22, the euhedral parts of this crystal have relatively magnesian glass adjacent to them, while the resorbed parts are next to glass with 7 percent MgO.

Iki-33 provides evidence that this same kind of heterogeneity was present almost to the end of the eruption. One grain, completely euhedral, is surrounded by glass identical to the distant glass. An adjacent resorbed grain is surrounded by glass with significantly less MgO. The cluster of euhedral grains shown in figure 25.6A-B lies in a pool of glass with 8 percent MgO; these grains show only minor resorption. A last grain, of class 1, is surrounded by a sheath of glass with 7.2 to 7.7 percent MgO and is strongly resorbed on all sides.

Similar patterns occur in the other eruption samples analyzed so far. The main variants may be summarized as follows:

(1) In the first type of rim-glass relationship, the adjacent glass contains 0.2 to 1.5 weight percent less MgO than the glass more than 1 mm away from olivine. The enclosed olivine shows signs of resorption, such as rounding of corners and wavy or cusped margins, as seen in figures 25.4E, 25.5A, and 25.13. Resorption may be partial, or the entire rim of the crystal may be affected. Glass next to resorbed surfaces is consistently less magnesian than glass adjacent to euhedral corners and edges, even on the same grain. A dozen such grains, partly or completely rimmed by low-MgO glass, have been found. They occur in samples Iki-7, 11, 9, 14, 20, 24, and 32, in addition to the samples in figure 25.12.

(2) In the second type of rim-glass relationship, the adjacent glass has a composition essentially equal (within ± 0.2 weight percent MgO) to that of the more distant glass. There is no correlation between crystal form and glass composition; the grain may be locally resorbed or completely euhedral. Thirty-one such grains have been analyzed, of which 12 are essentially euhedral.

In addition, there are two small euhedral grains, one in Iki-9 and the other in Iki-32, which have skins of low-MgO glass but show little resorption, like the cluster of grains in Iki-33 (fig. 25.6A-B). No cases are known in which an olivine grain has a sheath of glass appreciably more magnesian (>0.2 percent MgO) than the distant glass.

The existence of these boundary layers (or sheaths) of contrasting glass composition was not evident from petrographic examination, as no color difference exists between the various compositions; their presence was only detected with the microprobe. These MgO-poor boundary layers cannot simply result from quench overgrowth on olivine, because 31 out of 46 grains do not have them. Sheathed grains are not rare, though; they make up 30 percent of the grains analyzed. The possibility that olivine (or other) crystals might carry a boundary layer of melt with them as they move has been suggested before (Helz, 1980), but the layers themselves have not previously been observed.

COMPOSITION OF OLIVINE IN THE LAKE

The rapidly quenched eruption pumice samples preserve many sorts of disequilibrium and evidence of magma mixing. Olivine phenocrysts in the lake, by contrast, have had months or years to exchange Mg for Fe with the surrounding host liquids before being quenched during drilling. Table 25.5 presents data for olivine in the aggregates and megacrysts described in table 25.2. These grains differ from isolated phenocrysts in the same samples in that core compositions may be slightly more forsteritic, but they are otherwise quite representative of phenocrystic olivine in the lake.

The shallow samples (KI-113 and KI76-2-20.5 in table 25.5) show strong normal zoning, from Fo_{88-86} (cores) to Fo_{78-72} (rims). Such extensive zoning, with a range of 10-14 percent Fo, is unknown so far in the eruption samples. This zoning probably developed in the lake, during crystallization of the groundmass. Note that the holocrystalline sample (KI76-2-20.5), quenched from about 100 °C, shows more extensive zoning than the KI-113 clots, which was quenched from 1,090 °C. Extensive normal zoning of this sort is common in olivine phenocrysts in older Hawaiian lava flows (Maaloe and Hansen, 1982). In the flows, some uncertainty exists over whether the narrow, iron-rich rims are overgrowths or result from exchange of Fe and Mg between preexisting olivine and the differentiating melt. In these lake samples, there is no ambiguity; the zoning is produced by re-equilibration, not by overgrowth.

Samples from deeper in the lake show progressively less zoning, always in the normal sense. In KI67-2-87.9 (table 25.5) the range in forsterite content is 10 mol percent. The intragrain color variations seen in the olivine cluster in figure 25.8D are produced by this zoning. It is evident that the zoning follows the outline of the whole aggregate, not of individual grains within the cluster. In the 1981 samples (table 25.5, columns 5-6 and 9-10) the range of forsterite variation is only 4-5 mol percent. In these later samples, there is a positive correlation between maximum forsterite content and core quenching temperature, as follows:

Sample	Percent Fo	Temperature (°C)
KI81-1-238	85.1	1,135-1,140
KI67-2-87.9	82.7	1,090
KI81-1-181.5	79.2	1,010-1,030

Even more extensive re-equilibration of olivine phenocrysts has been described by Moore and Evans (1967) in samples from deep within the prehistoric Makaopuhi lava lake. There, the phenocrysts were almost unzoned and had the same composition as groundmass olivine. Maaloe and Hansen (1982) present calculations showing how zoning in initially forsteritic olivine phenocrysts would be expected to change with time, as exchange of Fe for Mg proceeds. The olivine in both lava lakes follows the model very well.

The feature of these data most relevant to the present paper, however, is that they suggest that even the largest olivine aggregates and megacrysts have been affected by exchange of Fe and Mg with the melt during slow cooling. The zoning complexities present in the eruption olivine phenocrysts are gone, even in the earliest drill core.

TABLE 25.5.—Composition of olivine megacrysts and grains in dunitic aggregates from Kilauea Iki lava lake, 1959 Kilauea eruption

Sample type	KI-113 class I aggregate		KI67-2-87.9 class I aggregate		KI81-1-181.5 mosaic		KI76-2-20.5 megacryst		KI81-1-238 megacryst	
	3	1	2	1	5	1	7	1	4	3
SiO ₂	39.61	37.53	39.82	38.14	38.52	37.87	39.70	37.18	39.68	38.8
TiO ₂	.00	.00	.04	.07	.00	.00	.00	.01	.00	.02
Al ₂ O ₃	.00	.00	.04	.06	.00	.00	.00	.00	.00	.01
Cr ₂ O ₃	.00	.00	.02	.03	.00	.00	.02	.00	.00	.00
FeO	11.93	21.95	16.20	24.83	19.54	23.26	12.88	25.08	14.12	18.19
NiO	.17	.04	-	-	.09	.11	.20	.11	.14	.02
MnO	.17	.32	.15	.21	.28	.33	.19	.34	.18	.25
MgO	47.03	39.47	43.62	36.74	41.79	38.55	46.49	37.17	45.29	42.30
CaO	.24	.24	.30	.28	.15	.17	.22	.20	.23	.29
Na ₂ O	.01	.00	.05	.07	.01	.01	.02	.01	.02	.02
Total percent	99.16	99.55	100.24	100.43	100.38	100.30	99.72	100.10	99.66	99.96
Mol percent Fo	87.5	77.8	82.7	72.51	79.2	74.7	86.6	72.5	85.1	80.6
Location	core largest grain in aggregate	rim	core large single crystal	rim	small grain, center of mosaic	rim of larger crystal at edge of aggregate	core	rim	core	rim
Quenching temperature (°C)	1090-1095°C		1090°C		1010-1030°C		~ 100°C		1135-1140°C	

Only the sizes and textures of the aggregates and megacrysts may preserve information relevant to the dynamics of the 1959 eruption.

DISCUSSION

The olivine phenocryst population in the 1959 eruption samples is very heterogeneous petrographically. It is somewhat more uniform chemically, but zoning patterns are varied, with normally and reversely zoned grains almost equally abundant in the population analyzed. There is no correlation between petrographic class and chemical composition. The petrographic and chemical characteristics of this olivine phenocryst population vary from phase to phase of the eruption, supporting a model of magma mixing and progressive internal equilibration that will be advanced below.

Olivine in Kilauea Iki lava lake retains all of the textures seen in the eruption samples. In addition to abundant olivine phenocrysts, the lake contains rare olivine megacrysts and dunitic aggregates. Though textures are stable for decades in the lake, chemical

composition is not. The lake olivines are all normally zoned, and their cores may be relatively Fe-rich, because of continued exchange of Fe and Mg with the melt during slow cooling of the lava lake.

Many features of this population of phenocrysts and aggregates are unusual and bear on the dynamics of the 1959 eruption. These features are (1) the presence of deformed olivine grains, (2) the presence of dense olivine aggregates of complex history, (3) the occurrence of rare olivines containing sulfide-bearing inclusions, (4) the presence of reversely zoned and of oppositely zoned crystals in a single thin section, and (5) the occurrence of resorbed olivine. The significance of these will be considered in turn.

DEFORMATION FEATURES IN OLIVINE

Olivine with multiple planar extinction discontinuities extending across the whole grain or with complex rectangular subgrains is present in the 1959 eruption pumice and in Kilauea Iki lava lake. The grains occur singly, in small clusters, or in larger aggregates.

Irregularly shaped, deformed crystals like this are common in Hawaiian alkalic rocks (see, among others, White, 1966). Similar kink-banded olivine, as isolated grains or in small clusters, has been reported from many other localities as well (Blanchard and others, 1976; Imsland, 1984; Francis, 1985). The kink-banded olivines are always among the coarsest grains present, as at Kilauea Iki. In most of these occurrences, the deformed grains are all very forsteritic (Fo_{90}), which is not the case in the 1959 pumice. Most authors consider the deformed olivine to be xenocrystic. Imsland (1984) considers it (and the chromian diopside associated with it in the ankaramites of Jan Mayen) to be mantle-level phenocrysts precipitated from the ankaramitic parental liquid.

Extinction discontinuities, or rectangular subgrain boundaries like those shown in figure 25.5B, have been produced experimentally in olivine at high temperatures and pressures (Raleigh, 1968; Carter and Ave Lallemand, 1970; Raleigh and Kirby, 1970). They form in olivine in a crystalline matrix, in response to non-hydrostatic stress. As yet there are no studies that investigate the minimum amount of interstitial melt necessary to prevent olivine from deforming in this manner. Kink-bands do not form under hydrostatic conditions, however; kink-banded crystals surrounded by melt (figs. 25.3, 25.4A–B) must have been deformed in a very different environment.

Aggregates of deformed olivine are the most numerous class of dense olivine aggregates in Kilauea Iki (table 25.2). The deformed olivine in these aggregates is similar in size and petrographic character to the isolated, deformed phenocrysts. It was suggested above that the isolated class 1 crystals were produced by disaggregation of coarse, mildly deformed dunite like the seven dense, melt-poor aggregates found in the lake. In fact, the literature on olivine deformation virtually requires such an origin for any grain with deformation features. Their depth of origin cannot be tightly constrained merely from the presence of deformation features, however, as olivine deforms readily over a wide range of pressures and temperatures. Nevertheless, minimum confining pressures of several hundred megapascals, much higher than the 100 MPa (1 kbar) in Kilauea's summit reservoir, seem indicated (Carter and Ave Lallemand, 1970).

DENSE OLIVINE AGGREGATES

Kilauea Iki lava lake contains several dense aggregates of olivine, as discussed above. Most consist of coarse, mildly deformed class 1 grains; others contain polygonal mosaics of unstrained olivine (table 25.2). Neither of these types contains significant amounts of basaltic melt, and where melt does occur, it appears to be the host melt penetrating the aggregate, rather than being indigenous to the aggregate. The mineralogy and textures of these aggregates are matched by those of the dunite tectonite xenoliths that are so common in Hawaiian mafic alkalic rocks, whether from the Honolulu Volcanics (Jackson and Wright, 1970), Hualalai (Kirby and Green, 1970), Loihi Seamount (Moore and others, 1982; Roedder, 1983), or elsewhere (White, 1966; Jackson, 1968). Similar textures occur in other types of olivine-rich xenoliths and in alpine peridotite (see,

for example, Mercier and Nicolas, 1975; Mercier, 1979). Textures like those seen in the coarse, mildly deformed aggregates of table 25.2 are considered by these authors to be produced by plastic deformation in the upper mantle, the polygonal mosaics by recrystallization of deformed grains and subsequent annealing. It seems possible that the textures of the Kilauea Iki aggregates were produced the same ways.

The olivine in the dunite tectonite xenoliths from Hawaiian alkalic rocks are more iron-rich than the olivine in most peridotite. Jackson and Wright (1970) give $Fo_{87.5-84}$ and Sen (1983) gives Fo_{90-81} for the olivine in the dunite xenoliths in the Honolulu Volcanics, while White (1966) reports Fo_{89-84} for all dunite xenoliths from the Hawaiian Islands. This range is similar to the range of compositions seen in class 1 olivines in the pumice samples ($Fo_{88.7-85}$) and to the core compositions seen in the dunitic aggregates in the lake ($Fo_{87.5-83}$). However, the same compositional range is observed for other classes of olivine phenocrysts in this eruption (fig. 25.9A) and for olivine from other Hawaiian tholeiite (Maaloe and Hansen, 1982; Basaltic Volcanism Study Project, 1981).

The origin of these relatively iron-rich dunite tectonites has been controversial. Their compositions and the fact that they tend to occur in lavas that have come up near the central conduit of tholeiitic shields (Jackson and Wright, 1970) suggest a relationship with the tholeiitic series, even though the dunite is normally found in alkalic rocks. They have been considered to be residual (Jackson and Wright, 1970) cumulates from shallow crustal magma chambers (Sen, 1983) or perhaps from the mantle (Wright, 1984), or metamorphic mantle rocks of indeterminate origin (Kirby and Green, 1980). None of these ideas explains simultaneously (1) the iron-rich olivine compositions identical to those of tholeiitic phenocrysts, (2) the general scarcity of minerals other than olivine + chromite, and (3) the absence of cumulate textures and the ubiquity of deformed or annealed textures in this rock type.

The model favored here is that the dunitic inclusions in the 1959 lava are cumulates from tholeiite, as suggested by Sen (1983) and Wright (1984), but that they precipitated on conduit walls at mantle and deep crustal levels, rather than in shallow crustal reservoirs. Their composition suggests they are cumulates from tholeiite, and their limited mineralogy suggests they formed in a thermally buffered environment. Heating of the conduit wall, by frequent passage of tholeiitic liquid, seems more likely to forestall precipitation of interstitial pyroxene and other minerals than periodic replenishment of more isolated, shallow crustal reservoirs. Also, the occurrence of similar dunite inclusions in summit lava of the very young volcano Loihi suggests that they start forming early in the development of the tholeiitic shield, and that at that stage they are already located very near the main conduit. Lastly the rarity of undeformed representatives of this type implies they come from an environment where low melt fractions and a plastic response to non-hydrostatic stress are the norm. These conditions are not likely to be met in shallow magma chambers. In this model, megacrysts like those found in Kilauea Iki would be presumed to form in melt-rich pockets along the conduit wall. Disruption of these pockets by a

later batch of magma would then incorporate the megacrysts into a magma capable of erupting.

By contrast with these dunite tectonites, the cumulate-textured xenoliths described by Jackson (1968) are much more likely candidates to be cumulates from crustal magma chambers of the sort visualized by Sen (1983). This suite contains minor dunite. Most of its representatives contain appreciable pyroxene and plagioclase, as well as olivine, in contrast to the dunite tectonites, which rarely contain other minerals. Also, the members of this suite, including its rare dunite, were described by Jackson (1968) as exhibiting no deformation features.

An alternate way of producing Fe-rich dunite tectonite might be to have the spinel-hercynite, typical of the Hawaiian upper mantle away from tholeiitic conduits (Jackson, 1968; Jackson and Wright, 1970) react completely with passing tholeiitic liquid, removing pyroxene and changing the composition of the remaining olivine + chromite. Whatever path was followed, it seems likely that the iron-rich, deformed dunite is produced at upper mantle or deep crustal levels, in the immediate vicinity of the tholeiitic conduit. The geochemistry of the included rare gases in some dunite tectonites is MORB-like (Kaneoka and others, 1983; Rison and Craig, 1983), which suggests they are associated somehow with the oceanic lithosphere that underlies all Hawaiian volcanoes, or at least, that they may have exchanged the isotopes with such material. The isotopic composition of the 1959 dunite samples is unknown, but after months or years of storage in the lake, they will not be pristine in any case.

The questions then arise of how the dunite is deformed, and what the timing of the deformation is, relative to the time of eruption. Mercier (1979) compared textures of xenoliths in kimberlite with experimentally observed rates of recrystallization for deformed olivine and concluded that at 1,400–1,600 °C the deformation textures, especially in kink-banded paleoblasts, would be entirely recrystallized within hours or days. For those xenoliths, he suggested that the textures must have been produced by the host kimberlite itself, as it moved through the mantle to the surface.

In the present case, it has been observed that deformed olivine grains have persisted for 22 years in the lava lake at 1,140–1,190 °C. The expected temperatures in the upper part of Kilauea's conduit and in the deeper parts of the shallow reservoir are probably 1,250–1,350 °C, based on estimates of parental MgO contents by Wright (1984) and the resulting liquidus temperatures suggested from the calibration of Helz and Thornber (in press). At these temperatures, the deformation features observed in single grains and in aggregates would be expected to survive for days to years, but beyond that their age cannot be constrained, as there are no data on static olivine-annealing rates in the temperature range of interest. Consequently, it is not possible to say that all of the deformation features seen in the 1959 olivine were produced by the host magma; at these lower temperatures, some may have been produced in earlier deformation events. Indeed the localization of chromite at grain boundaries in some aggregates where the coarsest olivine still contains deformation features (fig. 25.7C) may indicate that these aggregates have been subject to repeated deformation.

Nevertheless, the absence of primary igneous (cumulate) textures supports the idea that the dense aggregates come from an environment where deformation is almost unavoidable during sampling by the host, if not before. Furthermore, the scarcity of strongly deformed olivine or olivine aggregates in most Kilauea lava, including very olivine-rich shallow intrusives like the Uwekahuna laccolith, suggests that these dense aggregates have not formed in the shallow reservoir and do not survive there indefinitely. The more abundant glomerocrystic clusters of oriented, undeformed olivine, like that shown in figure 25.5A–B, are more likely representatives of olivine cumulates from Kilauea's shallow reservoir. The dense, deformed aggregates must have come from much deeper parts of Kilauea's plumbing.

The presence of two annealed aggregates (KI67.2–87.9b and KI81–1–181.5) containing no deformed grains complicates the picture somewhat. Their textures reflect prolonged thermal annealing in a hydrostatic environment. If the deepest parts of the conduit sampled are characterized by extremely low melt fractions and non-hydrostatic stress, these two aggregates must have been annealed at higher levels, suggesting that they were relatively high in the plumbing for some time prior to eruption.

SULFIDE-BEARING OLIVINE

Sulfides are rare in Kilauea basalt. They have been found included in, or associated with, ilmenite and titanomagnetite separates from differentiated rift lava (Desborough and others, 1968). They also occur as immiscible blebs in glass or as inclusions in augite in early scoria of the 1977 eruption (Moore and others, 1980), and as a late phase in interstitial liquid in Alae lava lake (Skinner and Peck, 1969) and in Kilauea Iki lava lake (R. T. Helz, unpub. data, 1985).

This paper reports the first known occurrence of sulfide in Kilauea summit lava. In the 1959 samples, it occurs in olivine as one phase in swarms of inclusions, which consist otherwise of chromite, glass, and vapor. This occurrence is very similar to the occurrence of sulfide as inclusions in olivine in the dunite xenoliths from Loihi (Roedder, 1983). Such grains and aggregates are very rare in the 1959 lava, and it was suggested above that they all came from the same limited source region.

The question is, where is that source? Sulfide is stable as a separate phase only at appropriate combinations of temperature, silicate melt composition, and sulfur and oxygen fugacities. The occurrence of sulfide as inclusions in some olivine phenocrysts demonstrates that the necessary combinations exist, at least locally, but the scarcity of sulfide-bearing melt inclusions in the 1959 and other summit lava suggests that the conditions are rarely met. It is known that melt composition and oxygen fugacity of Kilauea lava vary within rather narrow limits (Wright, 1971; Anderson and Wright, 1972). To the extent that magma temperatures of the 1959 lava were higher than most summit eruptions, the lava would be less likely than most to contain sulfide. One can conclude, therefore, that the sulfur fugacity was, at least locally, higher than usual. Recent studies of gases emitted from the summit area of Kilauea Volcano

show a tremendous flux of magmatic gas (CO_2 , SO_2), which is lost from stored magma even between eruptions (Greenland and others, 1985; Gerlach and Graeber, 1985). Most melt inclusions in olivine are sulfide-free, suggesting that the melt in the summit reservoir generally contains much less sulfur than would be required to stabilize a separate sulfide liquid. It seems likely, therefore, that the sulfide-bearing inclusions formed at greater depth than the other melt inclusions, either in the lowest parts of the summit reservoir or deeper. Geobarometry on the sulfide-bearing olivine, using the methods of Roedder (1983) or Harris and Anderson (1983), might help constrain the depth of origin of these and other olivine xenocrysts. The observations that the sulfide-bearing, inclusion-rich olivine almost never contains deformation features and that aggregates of such olivine tend to be less densely compacted (fig. 25.7D) than the deformed olivine aggregates are compatible with the idea that class 5 olivine is derived from higher levels than the deformed class 1 olivine and the dense aggregates. The presence of sulfide-bearing inclusions in one of the annealed aggregates (shown in fig. 25.8A–B) suggests that this particular aggregate was stored and annealed at a level close to the source of the other sulfide-bearing olivine, though this very dense aggregate may have originated at still greater depths.

SIGNIFICANCE OF OLIVINE ZONING IN THE ERUPTION PUMICE

A complete evaluation of olivine zoning in the 1959 lava must wait on the availability of detailed compositional profiles of the olivine. However, the isolated point analyses presented here are sufficient to characterize the nature and extent of zoning and its gross variation with time during the eruption.

The most curious feature of the olivine zoning is the presence of a substantial number of reversely zoned crystals. Mechanisms for producing reverse zoning in olivine include magma mixing and decompression at constant temperature. Crystals entrained in a hotter magma might develop more magnesian rims eventually, but the usual effect in the 1959 lava is partial resorption. Some of the reversely zoned crystals in the 1959 lava are perfectly euhedral (fig. 25.4C) and show no sign of resorption or any other kind of hiatus in crystal growth, suggesting that some other mechanism is involved. The analysis of van Kooten and Buseck (1978) suggests that reverse zoning in olivine forms when a water-bearing melt, saturated with olivine, undergoes isothermal decompression. This results in an increase in oxygen fugacity, an increase in the $\text{Fe}^{+3}/\text{Fe}^{+2}$ ratio, and hence an increase in the $\text{Mg}/\text{Mg} + \text{Fe}^{+2}$ ratio in olivine crystallizing from the melt. Their calculations showed that forsterite content would increase 3–5 percent for a 200-Mpa (2 kbar) drop in pressure, at 1,000 °C, for a melt containing 2.5 weight percent H_2O . The pressure effect in a dry magma has been determined by Takahashi and Kushiro (1983) and is much smaller: if Kilauea magma were completely dry, a 3 percent reversal in Fo content would record 2,500 MPa (25 kbar) of isothermal decompression. The amount of water in Hawaiian tholeiite is of the order of 0.3–0.6 weight percent H_2O (Moore, 1965), so a pressure drop of between 200–2,500 MPa (2–25 kbar) would be required to

produce the maximum reverse zoning seen in the 1959 eruption.

The question arises as to what stage of decompression might be recorded in the reversely zoned phenocrysts. Every crystal in the eruption pumice was moved from the level of Kilauea's shallow reservoir, which is 2–6 km below the summit of the volcano (Eaton, 1962; Ryan and others, 1981), to the surface, and so has undergone a pressure drop of roughly 100 ± 50 MPa (1 ± 0.5 kbar). If this were sufficient to produce detectable reverse zoning, then all phenocrysts would be reversely zoned; in fact, only some of them are (see figs. 25.9B, 25.11). Furthermore, the number of reversely zoned olivine grains and the extent of reverse zoning tended to decline as the eruption progressed (fig. 25.14A–B). The trends are irregular but suggest that the reverse zoning is neither stable in shallow storage nor being produced there. Those olivine grains showing pronounced reverse zoning were probably brought up by the 1959 magma from below the level of the shallow reservoir.

Another question of interest is, how long could the variable zoning seen in the eruption samples last before internal equilibrium would be restored? Detailed calculations for each sample are beyond the scope of this paper, but the calculations of Maaloe and Hansen (1982) suggest that the time interval is between a month and a year, for zoned margins typically 10–30 μm thick. This is compatible with the observations that (1) the kind of zoning changed, and internal equilibrium in the eruption samples increased perceptibly over the 5-week period of the eruption and (2) shallow lake samples quenched as little as 9 months later show only strong normal zoning, of a sort rarely seen in the eruption samples. Thus many of the olivine grains from eruption pumice analyzed here were quenched within weeks, or at most a few months, of the time their zoning was produced.

SIGNIFICANCE OF RESORBED OLIVINES

Partial resorption of olivine is widespread in the 1959 eruption pumice and has been noted by previous workers (Richter and Murata, 1966). Resorption textures, including cusped margins like those shown in figures 25.4A, D have been produced experimentally by Thornber and Huebner (1985); these are not simply unusual growth forms. This resorption occurs in samples quenched from 1,160–1,217 °C (see table 25.4), far above the incoming of pigeonite, which lies at 1,090–1,100 °C in the 1959 lava (Helz and Thornber, in press; unpub. data, 1985). Consequently, the resorption cannot be the result of a reaction relationship between olivine and liquid.

As discussed above, about 30 percent of the olivine grains analyzed from eruption samples are partly or completely enclosed in a sheath of glass significantly less magnesian than glass elsewhere in the same section. Glass next to resorbed edges is significantly less magnesian than glass next to euhedral parts of the same grain. That these MgO-depleted glass sheaths are not produced by quench overgrowths in olivine seems clear from the fact that 70 percent of the olivine grains are bordered by glass identical in composition to glass farther away from olivine.

These observations suggest that the resorption was produced as follows: Olivine crystals from a cooler part of the magma

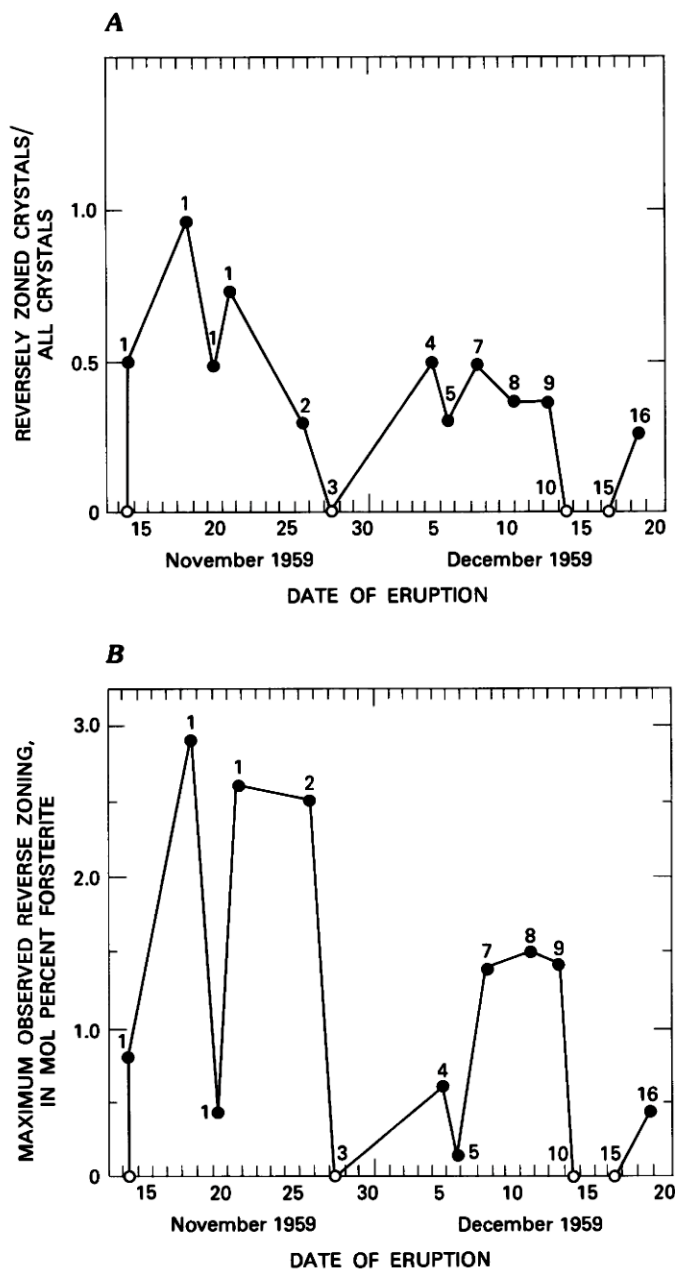


FIGURE 25.14.—Occurrence of reversely zoned olivine in 1959 eruption samples. **A**, Frequency of occurrence of reversely zoned crystals in 1959 eruption pumice, as a fraction of the total number of analyzed crystals, plotted against time of eruption. Points are labeled with the number of phase in which the sample was erupted. **B**, Maximum observed reverse zoning (as difference in mol percent F_o between core and rim) observed in 1959 eruption pumice, plotted against time of eruption. Samples containing no reversely zoned crystals plot on abscissa. Phase numbers as in figure 25.14A.

leading edge of the grain as it moves farther into the hotter liquid.) Thermal equilibrium between the new host and the crystal with its liquid boundary layer was established very rapidly (within minutes), at which point the melt in the boundary layer was superheated and no longer in equilibrium with olivine of any composition. The melt began to resorb the adjacent olivine, stopping when equilibrium was reached, that is, when the composition of the adjacent melt was equal to that of the rest of the melt. Once equilibrium was attained, the resulting odd-shaped grain persisted for decades without healing of the resorbed surfaces.

This model explains not only the occurrence of local resorption in olivine, but the fact that resorption is independent of rim composition or style of zoning. Of the 15 grains or clusters in low-MgO glass, 6 are normally zoned, 5 are unzoned, and 4 are reversely zoned. Rim compositions ranging from $F_{o88.0}$ to $F_{o80.7}$ have all been resorbed. This model also explains the occurrence of resorbed edges on 19 grains for which no compositionally distinct glass rims were found but which nevertheless show at least local resorption. Under this model, these would have had MgO-poor boundary layers at one time, but chemical equilibrium within the melt was re-established prior to quenching of the sample. The widespread occurrence of partial resorption of olivine in the 1959 samples implies that mixing of thermally disparate magmas was very common during the 1959 eruption.

These results have implications that may be important in other areas. First, resorption does not necessarily indicate that a given crystal is xenocrystic to the magma system. Second, one must be wary about calculating crystal-liquid distribution ratios in systems where magma mixing may have occurred, even where the glass is uniform in color, unless the glass has been thoroughly checked for chemical uniformity.

MODEL FOR THE 1959 ERUPTION

The physical processes preceding this eruption have been described by Eaton and Murata (1960), Eaton (1962), and Eaton and others (Chapter 48). In the late 1950's, seismic activity at Kilauea included intermittent swarms of deep (45–60 km) earthquakes. A minor swarm occurred in January 1959. The summit was inflating during the January swarm, and continued to do so thereafter, but subsided again between May and August 1959. This long period of subsidence was followed by an intense deep earthquake swarm on August 14–19. Re-inflation of the summit began in late September and continued until the outbreak of the eruption on November 14, 1959 (Eaton and Murata, 1960, fig. 7). Other precursory seismic activity included weak harmonic tremor at depths of 5–15 km, presumably resulting from upward migration of magma in the conduit. Beginning in September, shallow earthquakes occurred in the northern part of the caldera. These were numerous, but very small until November 14, just before the eruption. The seismic and tilt data combined to give a picture of magma, originating at 45–60 km, migrating upward and becoming lodged slightly to the north of Halemaumau, prior to triggering an eruption. The overall magma path was not unlike that outlined in Ryan and others (1981) for the period 1961–1974 at Kilauea. The 1958–1960

chamber were swept up in hotter, more mobile liquid. A thin layer of less magnesian, cooler, and hence slightly more viscous liquid moved with the crystals. (This layer might tend to gradually slough off the

period was exceptional, however, in having earthquakes at 45–60 km; such deep earthquakes have not been seen since. Also, the intense swarm of tiny earthquakes seen only on the north pit seismograph (Eaton, 1962; Eaton and others, chapter 48) are unique to the 1959 eruption.

Neither Eaton and Murata (1960) nor Eaton (1962) states specifically that the lava erupted in November and December 1959 included any of the magma liberated during the August earthquake swarm. It was not at first evident that this might be so, as can be seen by considering the usual pattern of magma storage in the summit reservoir (see Wright, 1971; and Wright and Fiske, 1971).

In these papers, it was shown that summit lava, though olivine controlled (Powers, 1955), typically lies at the olivine-depleted end of the olivine control line; that is, it contains minor phenocrystic olivine but has no fractionated augite or plagioclase. Variation in the amount of olivine, as observed in the 1959 eruption, was considered to be achieved by tapping different levels of a magma reservoir that was olivine-rich at the bottom and melt-rich at the top (Murata and Richter, 1966b; Wright, 1971).

In addition to varying in olivine content, the summit lava exhibits batch-to-batch compositional differences unrelated to olivine control. Different batches are chemically distinctive, some being unique, and can be followed through the volcanic plumbing. Wright and Fiske (1971) presented evidence that magma batches erupted at the summit in the 1950's and 1960's had appeared in flank eruptions 1–6 years earlier. They inferred that (1) magma batches arriving at the summit reservoir do not mix with each other in storage; (2) flank eruptions tap lower levels of the reservoir than summit eruptions do; and (3) summit eruptions usually tap magma that has been in storage in the shallow (2–4 km) reservoir for years, or even decades, prior to eruption.

Wright and Fiske (1971) recognized the 1959 eruption as exceptional in that neither of its two component magma batches (3a and 3b in the terminology of Wright and Fiske, 1971) had ever appeared in flank lava or as major eruptions in Halemauau. In particular, the 1960 Kapoho eruption, which immediately followed the 1959 summit eruption, was not related chemically to the summit eruption. The picture of the summit reservoir that emerged from this work was of a highly compartmentalized magma storage zone, like that shown by Fiske and Kinoshita (1969), such that even closely spaced eruptions might drain completely unconnected parts of the reservoir. This draining of discrete reservoirs has been demonstrated to occur at Kilauea during other time periods as well, including 1967–1969 (Dvorak and others, 1983) and 1972–1973 (Ryan and others, 1983). The isolation of the 1959 magma from all other parts of Kilauea's reservoir that were active from 1955 to 1965 led Wright and Fiske to hypothesize that the 1959 magma occupied chambers "separated from the main conduits of the central reservoir" (Wright and Fiske, 1971, p. 54).

Other exceptional features of this eruption, besides its unusual seismicity, chemistry, and inferred deviant path to the surface, include its having (1) the highest lava fountains observed at the summit (580 m, or 1,900 feet, observed December 17, 1959); (2) the hottest eruption temperatures ever measured (1,192 °C on

December 5, 1959); and (3) the most magnesian glass recovered for a historical Kilauea eruption. In addition, the pumice blanket produced during phase 3 is unusual in a historical Kilauea summit eruption. (All data is from Richter and others, 1970.) Thus, at least some of the 1959 lava was hotter and more gas-rich than typical Kilauea summit lava.

This paper has presented evidence that the 1959 lava contains material that appears to have originated below the level of the shallow reservoir. This includes (1) deformed olivine grains, singly and in aggregates, (2) aggregates of thermally annealed olivine, and (3) olivine megacrysts. Such materials are common in Hawaiian alkalic lava, but rare to absent in subaerial tholeiite, from Kilauea and elsewhere in Hawaii. In addition, the 1959 eruption contains rare olivine with sulfide-bearing inclusions and olivine with significant reverse zoning, neither of which appear to be produced in Kilauea's summit reservoir.

The unusual features of this eruption would be most easily explained if one of the two magmatic components erupted was the same magma that was liberated during the August earthquake swarm and reached the base of the shallow reservoir in late September. The hypothesis is that at that point the magma followed a seldom-used path to the north of the main reservoir (that is, the reservoir as located in Fiske and Kinoshita, 1969, and Ryan and others, 1981), encountering an older batch of stored magma. It broke through this older chamber to the surface on November 14, bringing some of the stored magma with it. The unusual features of the eruption are considered to be a direct consequence of the presence of the juvenile component.

THE MODEL AT MANTLE LEVELS

Kilauea tholeiite may originate as highly magnesian (>20 percent MgO) melt and fractionate appreciably, to MgO contents of 13–14 weight percent, enroute to the surface (Wright, 1984). The average MgO content of the 1959 eruption has been estimated as 15.43 percent (Wright, 1973) and hence is closer to the primitive melt than to the hypothesized parental one. Can this inferred differentiation from 20 to 15 percent MgO be made compatible with the apparent presence in the 1959 Kilauean lava of possible mantle-level material?

The answer to this potential contradiction is implicit in the theoretical model for the migration of fluid-filled cracks, as developed by Stevenson (1983), modifying earlier work by Weertman (1971a,b). In Stevenson's model, material from the lower end of the rising packet of fluid precipitates to close the crack below. In fact, healing the crack in this fashion is essential to migration of a discrete packet of melt. All that is necessary for a Kilauean tholeiite to contain mantle or deep crustal material and to differentiate is that the amount of material precipitated to seal the crack at the lower end exceed the amount picked off the walls at the upper end of the body of melt.

This model of crack migration dovetails with the hypothesized origin for the iron-rich dunite xenoliths proposed above. The dunite would correspond to this crack-healing material, because, for

TABLE 25.6.—Calculated settling velocities of olivine phenocrysts and aggregates in Kilauea Iki lava lake, assuming Newtonian behavior

Particle radius (cm)	Settling velocity (cm/s)
For viscosity 150 P, pressure 0.1 MPa (1 bar)	
0.25	0.05
0.5	0.21
1.0	0.85
For viscosity 50 P, pressure 1.5 GPa (15 kbar)	
0.25	0.16
0.5	0.65
1.0	2.6

tholeiite, the precipitate would be olivine + chromite. The exact composition of the olivine would vary slightly with depth, as the migrating melt fractionated enroute to the shallow reservoir. The deformation observed in the dunite xenoliths would be produced as the leading edge of a melt packet opened the crack, by analogy with the process Mercier (1979) inferred for deformed olivines in xenoliths in kimberlite. Because the Kilauea conduit is re-opened at frequent intervals, however, it is possible that some of the deformation observed in the dunitic aggregates was produced by an earlier packet of melt, not the host magma.

MAGMA ASCENT RATE

If the hypothesized model for the 1959 eruption is correct, we can calculate the average ascent velocity of the new magma package. To travel from depths of 45–60 km to the surface in the period from August 14–19 to November 14, the magma would have to move at 0.58–0.77 cm/s. This is compatible with ascent velocities for fluid-filled cracks, estimated by Stevenson (1983) to be 0.1–10 cm/s. It falls at the extreme low end of the range of ascent velocities Spera (1984) cites for xenolith-bearing lava (10^{-2} m/s to 30 m/s).

Is this velocity fast enough to entrain the largest objects found in the lake? Table 25.6 presents the results of calculating the Stokes' law settling velocities of olivine in basalt, for objects of different sizes. The first set of results is for a viscosity typical of very magnesian basalt at 0.1 MPa (1 atmosphere), the second set for the lower viscosity that the same melt would have at 1,500 MPa (15

kbar). Both viscosity estimates are taken from Kushiro and others (1976). The calculated settling rates for the largest particles found, which have average radii between 0.5 and 1.0 cm, would be 0.21–0.85 cm/s at low pressures and 0.65–2.6 cm/s at the high pressure limit. Non-Newtonian effects were neglected, on the assumptions that (1) much of the olivine phenocryst load (the very numerous class 2 olivine crystals and open aggregates) in the 1959 lava was in fact picked up from the lowest part of the older, stored magma, in Kilauea's summit reservoir and (2) the lava did not vesiculate until it was well up into the crust. The calculated Newtonian settling velocities are maximum values; to the extent that the magma was non-Newtonian, settling velocities would be lower, and the magma could more easily retain the larger olivine and olivine aggregates.

The calculated settling velocities are close to the average ascent velocity inferred above. If the eruption model is correct, this agreement means that the juvenile component was moving just fast enough to entrain the largest olivine and olivine aggregates found. It implies, further, that no significantly larger dunite inclusions will be found in the lake and that the magma never stopped moving from the time it picked up the aggregates until it began vesiculating, when non-Newtonian behavior took over. These deep-seated ascent rates are irrelevant to near-surface processes such as venting, fountaining, and so on, which involve the presence of a gas phase (see Eaton and others, chapter 48), resulting in strongly non-Newtonian behavior. The ability of the lava to entrain olivine in the shallow chamber was a function of magma discharge rate (Murata and Richter, 1966b); this rate increased during eruption, as the magma became more non-Newtonian (Wadge, 1981).

OLD VERSUS NEW MAGMA

It remains to be established which of the two recognized mixing components of the 1959 eruption was stored, old magma and which was the more juvenile. Early on it was noticed that the lava erupted from the east end of the initial fissure (Iki-58, or S-1 of Wright, 1973; or 3b of Wright and Fiske, 1971) was enriched in an augite-like component relative to west-end lavas (Iki-1 or S-2, or magma 3a). Murata and Richter (1966a) hypothesized that the former lava was derived by settling of augite phenocrysts into hotter parts of the magma chamber, where they were redissolved to give the east-end melt compositions. Calculations by Wright and Fiske (1971) supported this observation, though Wright (1973) noted that the implied physical model was very complex.

There are three problems with this augite-resorption hypothesis. First, it would require both components to be stored magma, rather than one stored and one juvenile, for if the Iki-1 (S-2) parent were not a stored component, the apparent relationship tested by the calculation would not exist, and the calculation would be meaningless. Second, the amount of augite (6 percent, Wright, 1973) required by the calculation is so small that the calculation cannot distinguish with certainty between low-pressure and high-pressure augite. Lastly, there is no petrographic evidence, in the form of phenocrystic augite, for the process. The tiny augite crystals

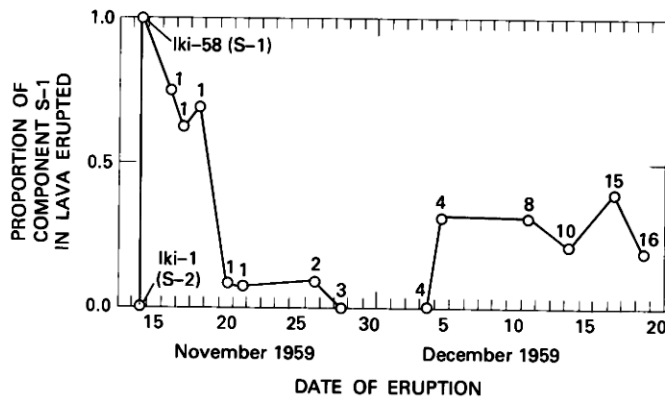


FIGURE 25.15.—Proportion of S-1 magmatic component present in various 1959 eruption samples (taken from Wright, 1973) plotted against date of eruption. The mixing components used by Wright (1973), namely samples Iki-58 (S-1) and Iki-1 (S-2), plot at 1.0 and zero respectively. Numbers by points identify the phase of the eruption.

in the initial eruption samples are not phenocryst-sized and are almost always associated with plagioclase. This is a problem because plagioclase is not required by the calculation, and augite could not be readily separated from plagioclase by flow differentiation of the sort described by Wright (1973). Careful search for augite phenocrysts in the lake, including samples of foundered crust and of the basal chill zone, has failed to uncover any phenocrystic augite, resorbed or otherwise; nor does augite occur as an inclusion in olivine in any eruption sample.

Another line of evidence that must be considered is shown in figure 25.15, which plots the change in mixing ratio found by Wright (1973) against time (see also Wright, 1973, fig. 3). Early phase 1 lava is disproportionately rich in S-1 (Iki-58, the east-end component), later phases richer in S-2 (west-end). This might be interpreted as showing that stagnant S-1 magma was pushed out first, as the chamber was flooded by new, hot S-2 magma.

However, three other lines of evidence favor the east-end lava (Iki-58 or S-1 or 3b) as the new component, with the west-end lava the stored component. The first is the recognition of Wright and Fiske (1971, p. 54) that the brief 1954 Halemaumau eruption was of west-end (their 3a) type. Thus, west-end lava had been in storage near the surface for five years prior to 1959. Second is the occasional recurrence of the west-end component in almost pure (>90 percent) form after the initial curtain of fire shrank to a single vent on November 15. Figure 25.15 shows that the late phase 1 and phase 3, and early phase 4 samples are pure, or nearly pure west-end (S-2) material. The east-end component is never seen in pure form, except of course in the type sample Iki-58, where its purity is a matter of definition only. This pattern is more compatible with east-end material being the newer material, seen only as it filters through older, stored magma.

The last piece of evidence that the east-end component may be the more juvenile is shown in figure 25.16, which shows the correlation between the amount of S-1 (east-end) material and

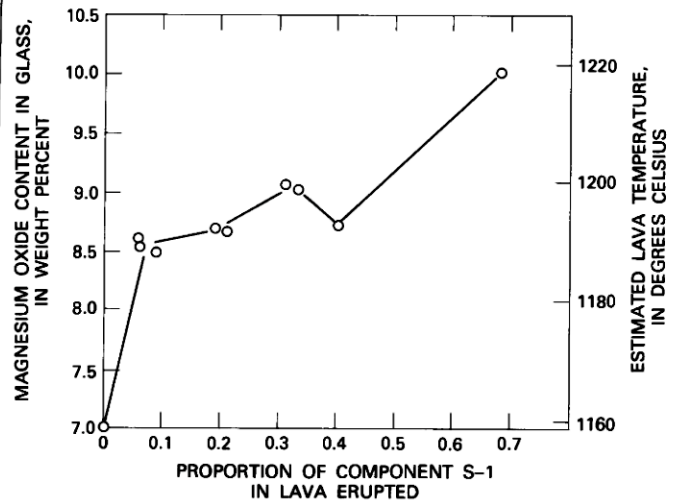


FIGURE 25.16.—MgO content of the glass (weight percent, left side) and estimated glass quenching temperature (right side) plotted against the fraction of S-1 component present for all samples erupted after November 17, for which both a bulk analysis and a glass analysis are available.

MgO content in glass (which covaries with temperature), for eruption samples from November 18 on. The more S-1, the hotter the sample, with the exception of Iki-32 from phase 15. This suggests that the S-1 component was consistently hotter than S-2 melts, hence probably more juvenile.

If one accepts that S-1 is the new and S-2 is the stored component, the above interpretation of the data in figure 25.15 must be revised. Instead of old magma being pushed out first, the new, more fluid magma must have streamed through the more stagnant material, to be erupted first. The stored magma was more prominent in later phases because it was remobilized by picking up heat and perhaps gas bubbles, from the newer, gassier material.

ERUPTION CHRONOLOGY

Using the above model and the data presented in this paper, the 1959 eruption can now be described in terms of progressively more intimate intermingling and internal equilibration of two separate types of olivine tholeiitic magma, a previously stored component and a new component that originated at 45-60 km depth and began its ascent in the August earthquake swarm.

The initial eruption fissure broke open along the south side of Kilauea Iki pit crater on November 14, 1959. Iki-1 (or S-2) was erupted at the west end, while Iki-58 (or S-1) was erupted at the east end. Initial samples of both components were relatively cool and differentiated, with a sparse population of class 2 olivine. Iki-58 is slightly hotter than Iki-1, however, and contains more phenocrystic olivine, including at least one reversely zoned grain (fig. 25.11), all features consistent with its being the new component. From November 14 to 17, lava continued to be dominantly east-end material (fig. 25.15), but gradually got hotter. On November 18, the hottest known sample, Iki-22, was erupted. This sample

contains a complex olivine assemblage that includes the most extensive reverse zoning found (tables 25.1, 25.3; figs. 25.11 and 25.14B).

No samples from November 19 have been analyzed, but by November 20, the lava being erupted was very nearly pure west-end material, though quite olivine-rich (fig. 25.15). The first such sample, Iki-44, contains a cooler glass than Iki-22, but the olivine is more magnesian and weakly zoned. Kink-banded olivine is present, but the banding is very faint, as the amount of deformation is slight. Compositionally, all the olivines appear to be in equilibrium with each other and (or) in equilibrium with a common melt. Such olivines might have come from the lowest (hottest) part of the west-end magma chamber.

A later sample from phase 1, Iki-7, is similar to Iki-44 in temperature in melt composition, and in the character of its class 1 olivines, but contains reversely zoned euhedral (class 2) olivines that are probably juvenile. Iki-7 also contains fragmental (class 4) olivine. Phase 2 (Iki-11) is slightly hotter and richer in the east-end component than Iki-44 and Iki-7. It contains the first normally zoned class 1 olivine found, the first sulfide-bearing class 5 olivine known, and more reversely zoned class 2 olivine. Clearly more new material was being tapped; the greater heterogeneity of the glass in Iki-11 (fig. 25.11) suggests that this mixing was very recent.

Phase 3 (Iki-9) was so extremely gas-rich that very little of it got into the lake; instead, it formed a pumice blanket downwind of the vent (Richter and others, 1970). It is pure west-end material, though slightly hotter than Iki-1 (S-2). Presumably this phase was derived from the gas-charged, differentiated upper part of the west-end magma chamber. The only puzzling feature of this phase is why this material did not erupt in phase 1. Two possible explanations are: (1) It came from an isolated cupola that was not breached by the initial fracture, or (2) the extra gas was derived from the new magma, which, after it had accumulated in a layer of differentiated west-end material near the roof, blew that material out as phase 3.

Early phase 4 lava was similar to that of phase 3. Later samples, like Iki-13, were much hotter (1,196 °C, table 25.4) and richer in east-end component (fig. 25.15) and olivine. The glass in Iki-13 is uniquely heterogeneous (fig. 25.11), suggesting that it was produced by very recent mixing of two components. Phase 5 (Iki-14) was hotter still (1,205 °C), but its glass is homogeneous, as though the disequilibrium of the Iki-13 mixing event had begun to dissipate. Both of these samples contain a complex assemblage (table 25.1) of very magnesian olivine (fig. 25.11) that shows little zoning. The combination of a change in mixing ratio of S-1 and S-2 (fig. 25.15), and the increase in temperature suggest that new material was fed into the base of the S-2 chamber about December 5. The presence of fragmental (class 4) olivine in these samples, presumably produced by brittle failure (shallow diking?), is compatible with this suggestion. The fact that both S-1/S-2 mixing ratios and glass quenching temperatures vary rather little after phase 5 suggests that this was the last significant influx of new material into the part of the chamber that was feeding the eruption.

Phase 7 (Iki-20) marks the reappearance of cooler lava (1,181 °C, see table 25.4). It also marks the first appearance of (1)

very diverse, non-overlapping core compositions within a single sample, and (2) convergence of olivine rim compositions from those very different cores toward a common rim composition. Earlier eruption samples, though exhibiting great diversity of zoning pattern, generally included only a narrow range of core compositions in classes 1, 3, 4, and 5 (taken together) and class 2 (see fig. 25.11). From phase 7 through phase 16, by contrast, one or both of these olivine groups include very varied phenocryst cores within a single thin section. These varied cores must have formed initially in different parts of the magmatic plumbing. Hence, their close juxtaposition in the later samples is evidence for increasingly intimate commingling of all parts of the active magmatic system. The convergent zoning suggests that this mingling resulted in accelerated internal equilibration of the samples. Rapid fine-scale mixing was possible because both components were basaltic and quite fluid, with only minimal viscosity contrasts.

Phases 8 and 9, represented by Iki-21 and Iki-24, include the last evidence for new material entering the actively erupting part of the chamber. They contain (1) the most magnesian olivine observed; (2) the only class 1 olivine with significant reverse zoning other than those in Iki-22 (figs. 25.11, 25.14B); and (3) the latest known fragmental olivine (table 25.1). The thermal perturbation at the onset of phase 8 (1,197 °C, compared with 1,181 °C in phase 7) is smaller than that at phase 4 (1,196 °C vs. 1,154 °C in phase 3), and Iki-24 (phase 9) is cooler still, rather than hotter, as Iki-14 (phase 5) was. This suggests that the amount of new material introduced was rather slight and may simply represent more thorough in-mixing of the deepest part of the chamber. On the other hand, these observations do agree with evidence presented by Eaton and others (chapter 48) that the magma reservoir was being intruded by new magma from the end of phase 1 through phases 8 and 9.

Subsequent samples from phases 10, 15, and 16, show some variation in the S-1/S-2 ratio but no thermal perturbations, suggesting that thermal equilibrium within the mixed volume was complete. Reverse zoning is scarce (figs. 25.11, 25.14A), and olivine rims are consistently iron-rich (fig. 25.11). Chemical equilibration was still incomplete, however, as evidenced by the occurrence even in phase 16 (Iki-33) of olivine with rims of low-MgO glass.

SUMMARY

This paper documents the petrographic and chemical diversity of the olivine phenocrysts and aggregates in the 1959 lava of Kilauea Volcano. The lava contains five petrographically distinct classes of olivine, dunitic aggregates with deformed or annealed textures, and two olivine megacrysts (10 × 20 mm in section). Olivine cores vary from Fo_{83.5} to Fo_{88.7}. Zoning is moderate (≤3 percent Fo within most crystals); normal and reverse zoning are about equally abundant. There is no correlation between petrographic class and core composition or style of zoning. Olivine in drill core from Kilauea Iki lava lake has the same petrographic features as olivine in the rapidly quenched eruption samples. Pre-eruption zoning and overall chemical composition is not preserved in the lake olivine, as it has

exchanged Mg for Fe with the melt.

Many features of the 1959 eruption are unusual for a historical Kilauea summit eruption and can be explained by a model in which one of the two observed magmatic components of this mixed-magma eruption came directly from the mantle, bypassing the main shallow reservoir. The component erupted from the east end of the initial fissure appears to be the juvenile component, responsible for the very hot, gas-rich, olivine-rich nature of the 1959 lava. The various components of the olivine population were picked up by the rising magma in roughly the following sequence:

(1) Deepest are the deformed olivine grains, aggregates of deformed olivine, and megacrysts, though the actual depths are poorly constrained. The thermally annealed aggregates may be strictly deep seated, or may have been annealed in shallower storage. All these materials are hypothesized to be derived originally from material lining the conduit wall at mantle or deep crustal levels. They are xenocrystic to the S-1 magma, but accumulated from earlier Kilauea tholeiite, so are not compositionally distinct.

(2) Euhedral olivine crystals with significant reverse zoning are deep-seated phenocrysts of the S-1 magma, recording large (several hundred MPa, or several kbar), but poorly constrained amounts of near-isothermal decompression. Reversely zoned class 1 olivine grains were picked off the walls deeper than unzoned class 1 olivine and erupted sooner after sampling, as this style of zoning is not stable in the shallow reservoir.

(3) Sulfide-bearing olivine grains and aggregates, rarely deformed and never showing reverse zoning, come from somewhere above the source of the deformed and (or) reversely zoned olivine, but below the shallow reservoir, where SO_2 is liberated from the magma. They may be cognate but are more probably xenocrystic to the S-1 magma.

(4) The occurrence of fragmental class 4 olivine, presumably formed by brittle failure, correlates fairly well with other indicators for episodes of influx of new S-1 liquid into the shallow chamber at the end of phase 1, and at phases 4-5 and 8-9. These fragments are hypothesized to result from fracture of old shallow olivine cumulates within the volcanic edifice.

(5) The bulk of the phenocrysts present, including most euhedral and rounded class 3 grains, unzoned or with some normal zoning, were picked up from the lower parts of the stored (S-2) magma. The widespread resorption observed in all classes of olivine is a consequence of mixing of thermally disparate melts at this stage.

(6) The small, euhedral olivine crystals with strong (8 percent Fo) normal zoning formed in the most rapidly cooled margin of the stored magma; they were only rarely sampled during the eruption.

Disequilibrium features present in the eruption samples include:

(1) the presence of heterogeneous glass (away from olivine); (2) the presence of boundary layers of MgO-poor glass near olivine; (3) the presence of reversely zoned, unzoned and (or) normally zoned olivine in the same thin section; (4) the presence of olivine with very different core compositions in the same section; and (5) the presence of olivine with different rim compositions in the same section. Comparison with other data (Maaloe and Hansen, 1982) suggests that the mixing event(s) recorded by these features took place weeks

before the eruption, or perhaps only within the 36 days of the eruption itself. Further analysis of these various indicators of change, or "geospeedometers," is deferred to a later paper.

The presence of kink-banded olivine is, by comparison, a relatively slow geospeedometer, as these deformation textures may last months to a few years at shallow-reservoir conditions. Their rarity in subaerial tholeiite, even picritic lava, suggests that they do not survive for decades in subsurface reservoirs, in contrast to their survival for 22 years in Kilauea Iki lava lake. However, deformed olivine occurs frequently in submarine east-rift lava of Kilauea. This suggests that some lower rift lava may move out laterally into the rift before reaching the shallow reservoir and so, like the 1959 lava, avoid prolonged shallow storage before their eruption. It would be of interest to search this submarine lava for the other types of deeper seated material found in the 1959 lava.

REFERENCES CITED

- Albee, A.L., and Ray, L., 1970, Correction factors for electron probe microanalysis of silicates, oxides, carbonates, phosphates, and sulfates: *Analytical Chemistry*, v. 42, p. 1408-1414.
- Anderson, A.T., Jr., and Wright, T.L., 1972, Phenocrysts and glass inclusions, and their bearing on oxidation and mixing of basaltic magmas, Kilauea Volcano, Hawaii: *American Mineralogist*, v. 57, p. 188-216.
- Basaltic Volcanism Study Project, 1981, Basaltic volcanism on the terrestrial planets: New York, Pergamon Press, Inc., 1,286 p.
- Bence, A.E., and Albee, A.L., 1968, Empirical correction factors for the electron microanalysis of silicates and oxides: *Journal of Geology*, v. 76, p. 382-403.
- Bence, A.E., Brande, S., Indelicato, G., and Allen, F., 1981, Analysis of trace and minor elements in rock-forming minerals using an automated electron microprobe: *Proceedings of the 8th International Conference on X-ray Optics and Microanalysis*, p. 538-548.
- Blanchard, D.P., Rhodes, J.M., Dungan, M.A., Rodgers, K.V., Donaldson, C.H., Brannon, J.C., Jacobs, J.W., and Gibson, E.K., 1976, The chemistry and petrology of basalts from leg 37 of the deep-sea drilling project: *Journal of Geophysical Research*, v. 81, p. 4231-4246.
- Carter, N.L., and Avé Lallemant, H.G., 1970, High temperature flow of dunite and peridotite: *Geological Society of America Bulletin*, v. 81, p. 2181-2202.
- Chen, C.-Y. and Frey, F.A., 1983, Origin of Hawaiian tholeiite and alkali basalt: *Nature*, v. 302, p. 785-789.
- Chouet, B., and Aki, K., 1981, Seismic structure and seismicity of the cooling lava lake of Kilauea Iki, Hawaii: *Journal of Volcanology and Geothermal Research*, v. 9, p. 41-56.
- Clague, D.A., 1982, Petrology of tholeiitic basalt dredged from Hualalai Volcano, Hawaii [Abs.]: *Eos*, v. 63, p. 1138.
- Desborough, G.A., Anderson, A.T., Jr., and Wright, T.L., 1968, Mineralogy of sulfides from certain Hawaiian basalts: *American Mineralogist*, v. 63, p. 636-644.
- Dvorak, J., Okamura, A., and Dieterich, J.H., 1983, Analysis of surface deformation data, Kilauea Volcano, Hawaii from October 1966 to September 1970: *Journal of Geophysical Research*, v. 88, p. 9295-9304.
- Eaton, J.P., 1962, Crustal structure and volcanism in Hawaii: *American Geophysical Union Geophysical Monograph*, v. 6, p. 13-29.
- Eaton, J.P., and Murata, K.J., 1960, How volcanoes grow: *Science*, v. 132, p. 925-938.
- Fiske, R.S., and Kinoshita, W.T., 1969, Inflation of Kilauea Volcano prior to its 1967-1968 eruption: *Science*, v. 165, p. 341-349.
- Fleet, M.E., and MacRae, N.D., 1983, Partition of Ni between olivine and sulfide and its application to Ni-Cu sulfide deposits: *Contributions to Mineralogy and Petrology*, v. 83, p. 75-81.

- Fleet, M.E., MacRae, N.D., and Herzberg, C.T., 1977, Partition of nickel between olivine and sulfides: a test for immiscible sulfide liquids: *Contributions to Mineralogy and Petrology*, v. 65, p. 191-197.
- Ford, C.E., Russell, D.G., Craven, J.A., and Fisk, M.R., 1983, Olivine-liquid equilibria: temperature, pressure, and composition dependence of the crystal/liquid cation partition coefficients for Mg, Fe²⁺, Ca and Mn: *Journal of Petrology*, v. 24, p. 256-266.
- Francis, D., 1985, The Baffin Bay lavas and the value of picrites as analogues of primary magmas: *Contributions to Mineralogy and Petrology*, v. 89, p. 144-154.
- Gerlach, T.M., and Graeber, E.S., 1985, The volatile budget of Kilauea Volcano. *Nature*, v. 313, p. 273-277.
- Greenland, L.P., Rose, W.I., and Stokes, J.B., 1985, An estimate of gas emissions and magmatic gas content from Kilauea Volcano: *Geochimica et Cosmochimica Acta*, v. 49, p. 125-130.
- Häkli, T., and Wright, T.L., 1967, The fractionation of nickel between olivine and augite as a geothermometer: *Geochimica et Cosmochimica Acta*, v. 31, p. 877-884.
- Hardee, H.C., Dunn, J.C., Hills, R.G., and Ward, R.W., 1981, Probing the melt zone of Kilauea Iki lava lake, Kilauea Volcano, Hawaii: *Geophysical Research Letters*, v. 8, p. 1211-1214.
- Harris, D.M., and Anderson, A.T., Jr., 1983, Concentrations, sources and losses of H₂O, CO₂, and S in Kilauean basalt: *Geochimica et Cosmochimica Acta*, v. 47, p. 1139-1150.
- Harte, Ben, 1977, Rock nomenclature with particular relation to deformation and recrystallization textures in olivine-bearing xenoliths: *Journal of Geology*, v. 85, p. 279-288.
- Helz, R.T., 1980, Crystallization history of Kilauea Iki lava lake as seen in drill core recovered in 1967-1979: *Bulletin Volcanologique*, v. 43-4, p. 675-701.
- , 1983, Diverse olivine population in lavas of the 1959 eruption of Kilauea Volcano, Hawaii [abs.]: *Eos*, v. 64, p. 900.
- , 1984, In situ fractionation of olivine tholeiite: Kilauea Iki lava lake, Hawaii [abs.]: *Geological Society of America Abstracts with Programs*, v. 16, p. 536-537.
- Helz, R.T., Banks, N.G., Casadevall, T.J., Fiske, R.S., and Moore, R.B., 1984, A catalogue of drill core recovered from Kilauea Iki lava lake from 1967-1979: U.S. Geological Survey Open File Report 84-484, 72 p.
- Helz, R.T., and Thornber, C.R., in press, Geothermometry of Kilauea Iki Lava Lake, Hawaii.
- Helz, R.T., and Wright, T.L., 1983, Drilling report and core logs for the 1981 drilling of Kilauea Iki lava lake (Kilauea Volcano, Hawaii) with comparative notes on earlier (1967-1979) drilling experiences: U.S. Geological Survey, Open File Report 83-326, 66 p.
- Hermance, J.F., and Colp, J.L., 1982, Kilauea Iki lava lake: geophysical constraints on its present (1980) physical state: *Journal of Volcanology and Geothermal Research*, v. 13, p. 31-61.
- Imsland, P., 1984, Petrology, mineralogy and evolution of the Jan Mayen magma system: Reykjavik, Visindafelag Íslandinga, Rit 43, Prentsmidjan Oddi, 332 p.
- Jackson, E.D., 1968, The character of the lower crust and upper mantle beneath the Hawaiian Islands: *International Geological Congress, 23d, Prague, Proceedings*, v. 1, p. 135-150.
- Jackson, E.D., Clague, D.A., Engleman, E., Friesen, W.B., and Norton, D., 1981, Xenoliths in the alkalic basalt flows from Hualalai Volcano, Hawaii: U.S. Geological Survey Open-File Report 81-1031.
- Jackson, E.D., and Wright, T.L., 1970, Xenoliths in the Honolulu Volcanic Series, Hawaii: *Journal of Petrology*, v. 11, p. 405-430.
- Jarosewich, E., Nelen, J.A., and Norberg, J.A., 1979, Electron microprobe reference samples for mineral analyses: *Smithsonian Contributions to the Earth Sciences*, v. 22, p. 68-72.
- Kaneoka, I., Takaoka, N., and Clague, D.A., 1983, Noble gas systematics for coexisting glass and olivine crystals in basalts and dunite xenoliths from Loihi Seamount: *Earth and Planetary Science Letters*, v. 66, p. 427-437.
- Kirby, S.H., and Green, H.W., II, 1980, Dunite xenoliths from Hualalai Volcano: evidence for mantle diapiric flow beneath the Island of Hawaii: *American Journal of Science*, v. 280-A, p. 550-575.
- Kushiro, I., Yoder, H.S., Jr., and Mysen, B.O., 1976, Viscosities of basalt and andesite melts at high pressure: *Journal of Geophysical Research*, v. 81, p. 6351-6356.
- Leeman, W.P., and Scheidegger, K.F., 1977, Olivine/liquid distribution coefficients and a test for crystal-liquid equilibrium: *Earth and Planetary Science Letters*, v. 35, p. 247-257.
- Luth, W.C., and Gerlach, T.M., 1980, Composition and proportions of major phases in the 1959 Kilauea Iki lava lake in December 1978 [abs.]: *Eos*, v. 61, p. 1142.
- Luth, W.C., Gerlach T.M., and Eichelberger, J.C., 1981, Kilauea Iki lava lake: April 1981 [abs.]: *Eos*, v. 62, p. 1073.
- Maaloe, S., and Hansen, B., 1982, Olivine phenocrysts of Hawaiian olivine tholeiite and oceanite: *Contributions to Mineralogy and Petrology*, v. 81, p. 203-211.
- Macdonald, G.A., 1944, The 1840 eruption and crystal differentiation in the Kilauean magma column: *American Journal of Science*, v. 242, p. 177-189.
- Melson, W.G., Vallier, T.L., Wright, T.L., Byerly, G., and Nelen, J., 1976, Chemical diversity of abyssal volcanic glass erupted along Pacific, Atlantic, and Indian Ocean seafloor spreading centers: *American Geophysical Union Geophysical Monograph*, v. 19, p. 351-368.
- Mercier, J.-C.C., 1979, Peridotite xenoliths and the dynamics of kimberlite intrusion, in *The mantle sample: inclusions in kimberlites and other volcanics: Proceedings of the Second International Kimberlite Conference*, v. 2, p. 197-212.
- Mercier, J.-C.C., and Nicolas, A., 1975, Textures and fabrics of upper mantle peridotites as illustrated by xenoliths from basalts: *Journal of Petrology*, v. 16, p. 454-487.
- Moore, J.G., 1965, Petrology of deep-sea basalt near Hawaii: *American Journal of Science*, v. 263, p. 40-52.
- Moore, J.G., Clague, D.A., and Normark, W.R., 1982, Diverse basalt types from Loihi Seamount, Hawaii: *Geology*, v. 10, p. 88-92.
- Moore, J.G., and Evans, B.W., 1967, The role of olivine in the crystallization of the prehistoric Makaopuhi lava lake, Hawaii: *Contributions to Mineralogy and Petrology*, v. 15, p. 202-223.
- Moore, R.B., Helz, R.T., Dzurisin, D., Eaton, G.P., Koyanagi, R.Y., Lipman, P.W., Lockwood, J.P., and Puniwai, G.S., 1980, The 1977 eruption of Kilauea Volcano, Hawaii: *Journal of Volcanology and Geothermal Research*, v. 7, p. 189-210.
- Muir, I.D., and Tilley, C.E., 1957, Contributions to the petrology of Hawaiian basalts 1. The picrite-basalts of Kilauea: *American Journal of Science*, v. 255, p. 241-253.
- Murata, K.J., and Richter, D.H., 1966a, Chemistry of the lavas of the 1959-60 eruption of Kilauea Volcano, Hawaii: U.S. Geological Survey Professional Paper 537-A, 26 p.
- , 1966b, The settling of olivine in Kilauean magma as shown by lavas of the 1959 eruption: *American Journal of Science*, v. 264, p. 194-203.
- Powers, H.A., 1955, Composition and origin of basaltic magma of the Hawaiian Islands: *Geochimica et Cosmochimica Acta*, v. 7, p. 77-107.
- Raleigh, C.B., 1968, Mechanisms of plastic deformation in olivine: *Journal of Geophysical Research*, v. 73, p. 5391-5406.
- Raleigh, C.B., and Kirby, S.H., 1970, Creep in the upper mantle: *Mineralogical Society of America Special Paper 3*, p. 113-121.
- Richter, D.H., Eaton, J.P., Murata, K.J., Ault, W.U., and Krivoy, H.L., 1970, Chronological narrative of the 1959-60 eruption of Kilauea Volcano, Hawaii: U.S. Geological Survey Professional Paper 537-E, 73 p.
- Richter, D.H., and Moore, J.G., 1966, Petrology of the Kilauea Iki lava lake, Hawaii: U.S. Geological Survey Professional Paper 537-B, 26 p.
- Richter, D.H., and Murata, K.J., 1966, Petrography of the lavas of the 1959-60 eruption of Kilauea Volcano, Hawaii: U.S. Geological Survey Professional Paper 537-D, 12 p.
- Rison, W., and Craig, H., 1983, Helium isotopes and mantle volatiles in Loihi Seamount and Hawaiian Island basalts and xenoliths: *Earth and Planetary Science Letters*, v. 66, p. 407-426.
- Roedder, E., 1983, Geobarometry of ultramafic xenoliths from Loihi Seamount, Hawaii, on the basis of CO₂ inclusions in olivine: *Earth and Planetary Science*

- Letters, v. 66, p. 369-379.
- 1984, Fluid inclusions: Reviews in Mineralogy, v. 12, 644 p.
- Ross, J.V., Avé Lallement, H.G., and Carter, N.L., 1980, Stress dependence of recrystallized-grain and subgrain size in olivine: *Tectonophysics*, v. 70, p. 39-61.
- Ryan, M.P., Blevins, J.Y.K., Okamura, A.T., and Koyanagi, R.Y., 1983, Magma reservoir subsidence mechanics: theoretical summary and application to Kilauea Volcano, Hawaii: *Journal of Geophysical Research*, v. 88, p. 4147-4181.
- Ryan, M.P., Koyanagi, R.Y., and Fiske, R.S., 1981, Modelling the three-dimensional structure of macroscopic magma transport systems: application to Kilauea Volcano: *Journal of Geophysical Research*, v. 86, p. 7111-7129.
- Schwindinger, K.R., Roppo, P.S., and Anderson, A.T., Jr., 1983, Synneusis of olivine phenocrysts into glomeroporphyritic clusters [abs.]: *Geological Society of America Abstracts with Programs*, v. 15, p. 682.
- Sen, G., 1983, A petrologic model for the constitution of the upper mantle and crust of the Koolau shield, Oahu, Hawaii, and Hawaiian magmatism: *Earth and Planetary Science Letters*, v. 62, p. 215-228.
- Skinner, B.J., and Peck, D.L., 1969, An immiscible sulfide melt from Hawaii: *Economic Geology Monograph*, v. 4, p. 310-322.
- Spera, F.J., 1984, Carbon dioxide in petrogenesis III: role of volatiles in the ascent of alkaline magma with special reference to xenolith bearing mafic lavas: *Contributions to Mineralogy and Petrology*, v. 88, p. 217-232.
- Stevenson, D.J., 1983, Magmatic transport by the migration of fluid-filled cracks [abs.]: *Eos*, v. 64, p. 848.
- Takahashi, E., and Kushiro, I., 1983, Melting of a dry peridotite at high pressures and basalt magma genesis: *American Mineralogist*, v. 68, p. 859-879.
- Thorner, C., and Huebner, J.S., 1985, Dissolution of olivine in basaltic liquids I: Experimental observations and applications: *American Mineralogist*, v. 70, p. 934-945.
- Van Kooten, G.K., and Buseck, P.R., 1978, Interpretation of olivine zoning: study of a maar from the San Francisco volcanic field, Arizona: *Geological Society of America Bulletin*, v. 89, p. 744-754.
- Wadge, G., 1981, The variation of magma discharge during basaltic eruptions: *Journal of Volcanology and Geothermal Research*, v. 11, p. 139-168.
- Wanamaker, B.J., and Evans, B., 1985, Experimental diffusional crack healing in olivine, in Schock, R.N., ed., *American Geophysical Union Monograph 31*: p. 194-210.
- Weertman, J., 1971a, Theory of water-filled crevasses in glaciers applied to vertical magma transport beneath oceanic ridges: *Journal of Geophysical Research*, v. 76, p. 1171-1183.
- 1971b, Velocity at which liquid-filled cracks move in the Earth's crust or in glaciers: *Journal of Geophysical Research*, v. 76, p. 8544-8553.
- White, R.W., 1966, Ultramafic inclusions in basaltic rocks from Hawaii: *Contributions to Mineralogy and Petrology*, v. 12, p. 245-314.
- Wright, T.L., 1971, Chemistry of Kilauea and Mauna Loa lava in space and time: U.S. Geological Survey Professional Paper 735, 40 p.
- 1973, Magma mixing as illustrated by the 1959 eruption, Kilauea Volcano, Hawaii: *Geological Society American Bulletin*, v. 84, p. 849-885.
- 1984, Origin of Hawaiian tholeiite: a metasomatic model: *Journal of Geophysical Research*, v. 89, p. 3233-3252.
- Wright, T.L., and Fiske, R.S., 1971, Origin of the differentiated and hybrid lavas of Kilauea Volcano, Hawaii: *Journal of Petrology*, v. 12, p. 1-65.
- Wright, T.L., and Okamura, R.T., 1977, Cooling and crystallization of tholeiitic basalt, 1965 Makaopuhi lava lake, Hawaii: U.S. Geological Survey Professional Paper 1004, 78 p.
- Zablocki, C.J., and Tilling, R.I., 1976, Field measurements of apparent Curie temperatures in a cooling basaltic lava lake, Kilauea Iki, Hawaii: *Geophysical Research Letters*, v. 3, p. 487-490.